ATOMKI PREPRINT

A/18 (1987)

HU ISSN 0231-245X

Electromagnetic properties of ^{6}Li in a cluster model with breathing clusters

A.T. Kruppa, R. Beck and F. Dickmann

Submitted to Phys. Rev. C
December 1986

Institute of Nuclear Research of the Hungarian Academy of Sciences
Debrecen, P.O.Box 51, H-4001, Hungary

Kiadja a
Magyar Tudományos Akadémia
Atommagkutató Intézete
A kiadásért és szerkesztésért felelős
Dr. Berényi Dénes, az intézet igazgatója
Készült a Kinizsi Szakszövetkezet
Nyomdájában

Electromagnetic properties of ^{6}Li in a cluster model with breathing clusters

A.T. Kruppa
Magyar Tudományos Akadémia Atommagkutató Intézete, Debrecen,
P.O. Box 51, H-4001 Hungary
and
Kernforschungszentrum Karlsruhe, Institut für Kernphysik III,
P.O. Box 3640, D-7500 Karlsruhe 1, FRG

R. Beck[+] and F. Dickmann[+]
Kernforschungszentrum Karlsruhe, Institut für Kernphysik III,
P.O. Box 3640, D-7500 Karlsruhe 1, FRG

PACS index: 21.60G, 21.10F, 21.10K, 23.20

Abstract: Electromagnetic properties of ^{6}Li are studied using a microscopic $(\alpha+d)$ cluster model. In addition to the ground state of the clusters, their breathing excited states are included in the wave function in order to take into account the distortion of the clusters. The generator coordinate calculations are free from the spurious centre-of-mass motion and arbitrary parameters. The cluster stability condition is satisfied. The elastic charge form factor F_{C0} is in good agreement with experiment up to momentum transfer 8 fm^{-2}. The discrepancy appearing at momentum transfer $q^2 > 8$ fm^{-2} must be attributed to the omission of the short range nucleon correlation. The ground state magnetic form factor F_{M1} and the inelastic charge form factor F_{C2}^* are also well described. The breathing excited states of d influence the behaviour of F_{C0} at high momentum transfer only, but they have an effect on F_{M1} and F_{C2}^* even at low momentum transfer.
The effect of the breathing states of α on the form factors proves to be negligable except at high momentum transfer.
The ground-state charge density, rms charge radius, the magnetic dipole moment and a reduced transition strength are also obtained in fair agreement with experiment.

1. Introduction

It has been noted several times that among the p-shell nuclei ^{6}Li shows an anomalous behaviour. In electron scattering the exceptional behaviour of ^{6}Li appears in that, its form factors cannot be described in the framework of the harmonic oscillator independent particle model consistently with the other p-shell nuclei.[1,2] Attempts were made to describe the form factors of ^{6}Li by using different oscillator width parameters for the s- and p-shell nucleons[1-3], configuration mixing[4-6] and a finite potential well for the average field.[7,8] On the other hand it turned out that, the substantial residual two-body interaction present in ^{6}Li gives rise to short and long range correlation between the nucleons of ^{6}Li.[6-11] Furthermore, ^{6}Li has proved to be the best cluster nuclei[12] and a huge amount of work has been devoted to the understanding of its cluster structure. It has been confirmed that the states of ^{6}Li can be interpreted in terms of an alpha (α) and a deuteron (d) cluster and the other two- and three-cluster structures play only a minor role.[13,14]

The charge form factors of ^{6}Li has also been studied by an approach that differs essentially from the fully microscopic shell and cluster models. ^{6}Li was described by the motion of three structureless point particles but the composite nature of α was approximately taken into account

by the aid of forbidden states.[15,16] The three body problem was solved variationally or the exact Fadeev equations were considered.

In a previous paper[17] we introduced a cluster model in which the distortion effects of the clusters were studied by using a generator coordinate (GC) -type trial wave function in which, in addition to the intercluster separation, the oscillator width parameters of the clusters are treated as GC's. This amounts to improving the description of the ground states of the clusters and including, in the model, their breathing excitations. The specific (i.e. non-Pauli) distortion of the clusters is particularly important in an $(\alpha+d)$-type cluster model description since in the loosely bound deuteron cluster can easily be distorted.

The effect of the specific distortion of the deuteron has been thoroughly investigated in the αd elastic scattering process.[18-25] However, there are relatively few papers concerned with similar analyses of the electromagnetic properties of the bound $(\alpha+d)$ system. Since the pioneering work of Kudeyarov et al.[26], non-dynamical microscopic harmonic oscillator cluster models have been widely used in the description of electron scattering from ^{6}Li.[27-31] Such a consistent phenomenological approach has been recently developed.[32] In this work the original cluster model has been modified so as to allow the deuteron to be

deformed. In spite of the success of the phenomenological description better understanding of the structure of ^{6}Li requires dynamical cluster models i.e. cluster models based on the nucleon-nucleon (NN) interaction. Having solved the equation of the motion for the approximate wave function we may turn to the calculation of the matrix element of the electromagnetic multipole operators. Dynamically determined cluster model wave function were used in the Refs. 23,24 and 33-37 in the calculation of electromagnetic properties of ^{6}Li. However in these calculations the α particle is kept undistorted and for the deuteron only a few excited states are included. In Ref. 23 it was pointed out that "one must obviously try to calculate with a more flexible deuteron wave function".

In this work our aim is to study the effect of reasonably complete sets of breathing excited states of both the alpha and the deuteron cluster on the electromagnetic properties of ^{6}Li. Essentially similar calculations have recently been published for ^{7}Li.[38,39] The ground state properties we calculated are the charge monopole and the magnetic dipole form factors, the charge density distribution, and rms charge radius while the calculated excitation properties are the reduced transition strength and the inelastic charge quadrupole form factor for the transition leading to the first excited state of ^{6}Li.

The structure of the paper is the following. In the next section the cluster model with breathing clusters as applied to ^{6}Li is breafly reviewed. In Sect. 3. some standard formulas of the theory of the electron scattering are summarized and the procedure of calculating the GC kernels of the electromagnetic multipole operators is shown. The numerical results for the free clusters as well as for ^{6}Li are presented in section 4.

2. Breathing cluster model of ^{6}Li

The cluster model wave function of ^{6}Li is constructed from harmonic oscillator shell model states of the constituent clusters. The Slater determinant of the lowest shell model configuration of cluster c ($c = \alpha$ or d)

$$\Phi_c(M_c,\beta_c) = \mathcal{A}_c\left(\prod_{i=1}^{A_c}\phi(\underset{\sim}{r}_i,\beta_c)\cdot\sum_c\right) \qquad (2.1)$$

contain harmonic oscillator single-particle orbits of width parameter β_c ,

$$\phi(\underset{\sim}{r},\beta) = \left(\frac{\beta}{\pi}\right)^{3/4}\exp\left\{-\beta\underset{\sim}{r}^2/2\right\} \qquad (2.2)$$

and appropriate spin-isospin functions $\sum_c$. The symbol M_c is the z component of the cluster angular momentum. The fixed quantum numbers of the clusters (total angular momentum, orbital momentum, spin and isospin) are sup-

pressed for brevity. The antisymmetrization operator of the system c containing A_c nucleons is

$$\mathcal{A}_c = \frac{1}{(A_c!)^{1/2}} \sum_{\xi} (-)^{\xi} P_{\xi} \qquad (2.3)$$

where P_ξ is the permutation operator and $(-)^\xi$ is 1 for even and -1 for odd permutations.

In our GC method an unprojected basis function of ^{6}Li reads

$$\Psi(M_\alpha M_d, \beta_\alpha \beta_d, \underset{\sim}{\xi}\underset{\sim}{\zeta}) = \mathcal{A}_{\alpha d}\left(\Phi_\alpha(M_\alpha, \beta_\alpha, \underset{\sim}{\xi}_\alpha)\, \Phi_d(M_d, \beta_d, \underset{\sim}{\xi}_d)\right) \qquad (2.4)$$

where the intercluster antisymmetrizer is

$$\mathcal{A}_{\alpha d} = \left[\frac{A_\alpha!\, A_d!}{(A_\alpha + A_d)!}\right]^{1/2} \left(1 + \sum_{\xi'} (-)^{\xi'} P_{\xi'}\right) \qquad (2.5)$$

and $P_{\xi'}$ is a permutation operator between α and d. The form of the wave functions $\Phi_c(M_c, \beta_c, \underset{\sim}{\xi}_c)$ is similar to Eq. (2.1):

$$\Phi_c(M_c, \beta_c, \underset{\sim}{\xi}_c) = \mathcal{A}_c\left(\prod_{i=1}^{A_c} \varphi(\underset{\sim}{r}_i, \beta_c, \underset{\sim}{\xi}_c)\, \chi_\sigma\right) \qquad (2.6)$$

but the harmonic oscillator orbits involved are centred at $\underset{\sim}{\xi}_c$ instead of the origin:

$$\varphi(\underset{\sim}{r}, \beta, \underset{\sim}{\xi}) = \left(\frac{\beta}{\pi}\right)^{3/4} \exp\left\{-\beta(\underset{\sim}{r} - \underset{\sim}{\xi})^2/2\right\} \qquad (2.7)$$

In eq. (2.4) we used the relative and average position vector of the oscillator centres

$$\underset{\sim}{\zeta} = \underset{\sim}{\xi}_\alpha - \underset{\sim}{\xi}_d$$
$$\underset{\sim}{\xi} = \frac{1}{A_\alpha + A_d} \cdot \left[A_\alpha \underset{\sim}{\xi}_\alpha + A_d \underset{\sim}{\xi}_d\right] \qquad (2.8)$$

To proceed, we define translational invariant states. The projecting of internal states $\Phi_c^{int}(M_c, \beta_c)$ out of the wave function (2.1) is unambiguos. To get intrinsic states from (2.4) integration over $\underset{\sim}{\xi}$, which is presumably the simplest method is chosen[40]

$$\Psi^{int}(M_\alpha M_d, \beta_\alpha \beta_d, \underset{\sim}{\zeta}) = \int d\underset{\sim}{\xi}\, \Psi(M_\alpha M_d, \beta_\alpha \beta_d, \underset{\sim}{\zeta}\underset{\sim}{\xi}) \qquad (2.9)$$

The function (2.9) may be written in a form imitating the resonating group ansatz

$$\Psi^{int}(M_\alpha M_d, \beta_\alpha \beta_d, \underset{\sim}{\xi}) = \mathcal{A}_{\alpha d}\left(\Phi_\alpha^{int}(M_\alpha, \beta_\alpha)\, \Phi_d^{int}(M_d, \beta_d)\, \chi(\underset{\sim}{R}_{\alpha d}, \beta_\alpha \beta_d, \underset{\sim}{\xi})\right) \qquad (2.10)$$

where the wave function of the relative motion is

$$\chi(\underset{\sim}{R}_{\alpha d}, \beta_\alpha \beta_d, \underset{\sim}{\zeta}) = \left(\frac{\pi}{2\beta_\alpha + \beta_d}\right)^{3/2} \exp\left\{-\frac{1}{2}\, \frac{4\beta_\alpha \beta_d}{2\beta_\alpha + \beta_d} (\underset{\sim}{R}_{\alpha d} - \underset{\sim}{\zeta})^2\right\} \qquad (2.11)$$

$\underset{\sim}{R}_{\alpha d} = \underset{\sim}{R}_\alpha - \underset{\sim}{R}_d$ and $\underset{\sim}{R}_c$ is the centre of mass of cluster c.

Finally, it remains to give the basis function of good total angular momentum JM. First the relative orbital angular momentum $\mathcal{L}M$ between the α and d clusters is projected out by the help of the method given in Refs. 17 and 41.

$$\Psi^{int}(M_\alpha M_d, \beta_\alpha \beta_d, \mathcal{L}M, \underset{\sim}{\zeta}) = \int d\hat{\underset{\sim}{\xi}}\, Y_{\mathcal{L}M}(\hat{\underset{\sim}{\xi}})\, \Psi^{int}(M_\alpha M_d, \beta_\alpha \beta_d, \underset{\sim}{\zeta}) \qquad (2.12)$$

The total-angular-momentum-projected function emerges from the coupling of the orbital momentum $\mathcal{L}$ with the spin of the deuteron, which is the total-spin (I) of the system.

$$\Psi^{int}(\beta_\alpha\beta_d, JM_J, \tau) = \sum_{M_L M} \langle L M \,|\, M_L\, | JM\rangle \Psi^{int}(M_\alpha M_d, \beta_\alpha \beta_d, LM, \tau) \quad (2.13)$$

The wave function (2.13) is viewed as a generating function with τ as well as β_α and β_d being the generator coordinates. So the trial wave function of ^{6}Li looks like

$$\Psi^{int}(JM) = \sum_{i=1}^{N_\alpha}\sum_{j=1}^{N_d} \int d\tau\, f_{ij}(JM, \tau)\Psi^{int}(\xi_\alpha^i \beta_d^j, JM, \tau) \quad (2.14)$$

The GC amplitudes $f_{ij}(JM,\tau)$ of Eq. (2.14) are determined by the variational principle

$$\delta E = \delta\left(\langle\Psi^{int}|H|\Psi^{int}\rangle / \langle\Psi^{int}|\Psi^{int}\rangle\right) = 0 \quad (2.15)$$

where the Hamiltonian has the form

$$H = -\frac{\hbar^2}{2M}\sum_i \Delta_{r_i} + \sum_{i<j} V_{ij}(r_i - r_j) - T_{CM} \quad (2.16)$$

Here V_{ij} stands for the NN interaction and T_{CM} is the kinetic energy operator of the centre of mass. Using the ansatz (2.14) in Eq. (2.15) we get the Griffin-Hill-Wheeler integral equation

$$\sum_{i=1}^{N_\alpha}\sum_{j=1}^{N_d} \int d\tau'\left(H_{ij,i'j'}(\tau,\tau') - E\cdot N_{ij,i'j'}(\tau,\tau')\right) f_{i'j'}(JM,\tau') = 0 \quad (2.17)$$

where the Hamiltonian and overlap kernels are

$$H_{ij,i'j'}(\tau,\tau') = \langle\Psi^{int}(\beta_\alpha^i \beta_d^j, JM,\tau)\,|H|\,\Psi^{int}(\beta_\alpha^{i'}\beta_d^{j'}, JM,\tau')\rangle \quad (2.18)$$

$$N_{ij,i'j'}(\tau,\tau') = \langle\Psi^{int}(\beta_\alpha^i \beta_d^j, JM,\tau)\,|\,\Psi^{int}(\beta_\alpha^{i'}\beta_d^{j'}, JM,\tau')\rangle$$

This procedure implies that the width parameter values are fixed. Their actual values are to be selected carefully. They are determined by the stability condition, for the free clusters, whose importance is emphasized in the literature.[39] The wave function of the free cluster c is taken in the following form

$$\Psi_c^{(\rho)}(M_c) = \sum_{i=1}^{N_c} f_c^{i,\rho}\cdot \Phi_c^{int}(M_c, \beta_c^i) \quad (2.19)$$

The symbol ρ distinguishes different orthogonal states of c (ρ=1 corresponds to the ground state). The widths β_c^i and amplitudes $f_c^{i,\rho}$ are determined by minimizing the energy mean value of the c-cluster Hamiltonian. These optimum values of β_c^i are adopted for ^{6}Li as well.

Using the cluster states (2.19) the trial wave function (2.14) can be written in a more physical form

$$\Psi^{int}(JM) = \sum_{\rho=1}^{N_\alpha}\sum_{\rho'=1}^{N_d}\sum_{M_d M} \langle L M\,|\,M_d\,|JM\rangle\cdot \mathcal{A}_{\alpha d}\left(\Psi_\alpha^{(\rho)}(M_\alpha)\right.$$
$$\left.\Psi_d^{(\rho')}(M_d)\,\chi(R_{\alpha d}, JM, L)\right) \quad (2.20)$$

where

$$\chi(R_{\alpha d}, JM) = \sum_{i=1}^{N_\alpha}\sum_{j=1}^{N_d} t_\alpha^{i,\rho}\, t_d^{j,\rho'} \int d\tau\, f_{ij}(JM,\tau)\int d\hat{\xi}\, Y_{LM}(\hat{\xi})\cdot$$
$$\cdot\,\chi(R_{\alpha d}, \beta_\alpha\beta_d, \xi) \quad (2.21)$$

and the coefficients $t_c^{i,\rho}$ arise from the inversion of eq. (2.19) i.e.

$$\Phi_c^{int}(M_c, \beta_c^i) = \sum_{\rho=1}^{N_c} t_c^{i,\rho}\,\Psi_c^{(\rho)}(M_c) \quad (2.22)$$

In addition to the ground state, the ansatz (2.19) produces N_c-1 pseudostates which may be interpreted as the breathing modes. In the case of the α particle the first excited model state may be identified with the actually observed breathing mode at an excitation energy 20.1 MeV.

The inclusion of the excited cluster states in the sum (2.20) may take into account the specific distortion effects of the clusters. In order to study the influence of the cluster distortion, restricted calculations were also carried out. In these one or both of the clusters are only represented by their ground states. We will denote full calculations with $D_\alpha D_d$ (D standing for distortion) and restricted calculations in which the excited states of α, d and both are excluded by $G_\alpha D_d$, $D_\alpha G_d$ and $G_\alpha G_d$ (G standing for 'ground states' only), respectively.
In addition to these models, called manywidth models (MW), two simpler models are also considered: that in which the clusters have one common width parameter (CW) and that in which the clusters have two different single width parameters (DW). In the first case the common width parameter is selected by minimizing the sum of the intrinsic energies of α and d.

In order to study the force dependence of the results, three effective central NN interactions were employed: the Volkov force no.2 [42] (V2), the Brink-Boeker force B1[43] (BB1)

given in the form

$$V_{ij}(\underset{\sim}{r}_i-\underset{\sim}{r}_j)=\sum_k V_k(\underset{\sim}{r}_i-\underset{\sim}{r}_j)\left[W_k+M_k P_\sigma+B P_\sigma-H P_\tau\right] \qquad (2.23)$$

and the central part of the Minnesota force[44] (MN) which has the form as

$$V_{ij}(\underset{\sim}{r}_i-\underset{\sim}{r}_j)=\left(V_R(\underset{\sim}{r}_i-\underset{\sim}{r}_j)+\tfrac{1}{2}V_t(\underset{\sim}{r}_i-\underset{\sim}{r}_j)[1+P_\sigma]+\tfrac{1}{2}V_s(\underset{\sim}{r}_i-\underset{\sim}{r}_j)[1-P_\sigma]\right)\cdot \left(\tfrac{1}{2}u+\tfrac{1}{2}(2-u)P_\sigma\right) \qquad (2.24)$$

where P_σ, P_σ and P_τ are the space, spin and isospin exchange operators, respectively, and we set $W_k+M_k+B_k+H_k=1$. The spatial dependence of the nucleon-nucleon interaction used is pure gaussian. The Coulomb interaction is taken into account by a gaussian expansion.[45]

3. Generator coordinate description of electromagnetic properties

3.1 Formulas of the theory of electron scattering

In a plane-wave Born approximation neglecting the electron mass the cross section for unpolarized electron scattering from a nucleus with mass M_i may be written[46,47] as

$$\sigma(\theta)=\frac{\sigma_M}{1+\frac{2E}{M_i c^2}\sin^2\theta/2}\cdot\left[\frac{q_\mu^4}{q^4}F_L^2(q^2)+\left(\frac{1}{2}\frac{q_\mu^2}{q^2}+\operatorname{tg}^2\frac{\theta}{2}\right)F_T^2(q^2)\right] \qquad (3.1)$$

where θ is the scattering angle and the Mott cross section

$$\sigma_M=\left(\frac{Ze}{2E}\right)^2\frac{\cos^2\theta/2}{\sin^4\theta/2} \qquad (3.2)$$

describes electron scattering from the Coulomb field of a point charge Ze. The quantity $q_\mu=(p_\mu-p'_\mu)/\hbar=(\omega/\hbar c, \underset{\sim}{q})$ is the four-momentum transfer divided by $\hbar$, where the incident and scattered four-momenta of the electron are $p_\mu=(E/c, \underset{\sim}{p})$ and $p'_\mu=(E'/c, \underset{\sim}{p}')$. The longitudinal and transverse form factors $F_L^2(q^2)$ and $F_T^2(q^2)$ can be expanded in terms of multipole components

$$F_L^2(q^2)=\sum_{\lambda=0}^{\infty}|F_{C\lambda}(q)|^2=\frac{1}{2J_i+1}\frac{4\pi}{Z^2}\sum_{\lambda=0}^{\infty}|\langle J_f\|T^C_\lambda(q)\|J_i\rangle|^2 \tag{3.3}$$

and

$$F_T^2(q^2)=\sum_{\lambda=1}^{\infty}\left(|F_{M\lambda}(q)|^2+|F_{E\lambda}(q)|^2\right)=\frac{1}{2J_i+1}\frac{4\pi}{Z^2}\sum_{\lambda=1}^{\infty}\left(|\langle J_f\|T^M_\lambda(q)\|J_i\rangle|^2+|\langle J_f\|T^E_\lambda(q)\|J_i\rangle|^2\right) \tag{3.4}$$

here $|J_i\rangle$ and $|J_f\rangle$ are the initial and final nuclear states with total angular momentum J_i and J_f, respectively.

The Coulomb, transverse magnetic and transverse electric multipole operators are related to the charge and current density operators $\rho(\underset{\sim}{r})$ and $\underset{\sim}{J}(\underset{\sim}{r})$ of the nucleus by

$$T^C_{\lambda\mu}(q)=\int d\underset{\sim}{r}\; j_\lambda(qr)Y_{\lambda\mu}(\hat{\underset{\sim}{r}})\rho(\underset{\sim}{r}) , \tag{3.5}$$

$$T^E_{\lambda\mu}(q)=\frac{1}{q}\int d\underset{\sim}{r}\;\underset{\sim}{\nabla}\times\left(j_\lambda(qr)\underset{\sim}{Y}^{\mu}_{\lambda\lambda1}(\hat{\underset{\sim}{r}})\right)\cdot\underset{\sim}{J}(\underset{\sim}{r}) \tag{3.6}$$

and

$$T^M_{\lambda\mu}(q)=\int d\underset{\sim}{r}\; j_\lambda(qr)\underset{\sim}{Y}^{\mu}_{\lambda\lambda1}(\hat{\underset{\sim}{r}})\cdot\underset{\sim}{J}(\underset{\sim}{r}) \tag{3.7}$$

where j_λ, $Y_{\lambda\mu}$ and $\underset{\sim}{Y}^{\mu}_{\lambda\lambda1}$ are the spherical Bessel function, spherical harmonics and vector spherical harmonics respectively. If the charge and current density operators of the nucleus are taken to be sums of the corresponding free densities of point-like nucleons, the multipole operators become

$$T^C_{\lambda\mu}(q)=\sum_i e_i\, j_\lambda(qr_i)Y_{\lambda\mu}(\hat{\underset{\sim}{r}}_i) \tag{3.8}$$

$$T^M_{\lambda\mu}(q)=\sum_i\frac{c\hbar}{Mc}q\left\{\left[-\left(\frac{\lambda}{2\lambda+1}\right)^{1/2}j_{\lambda+1}(qr_i)\underset{\sim}{Y}^{\mu}_{\lambda\lambda+1}(\hat{\underset{\sim}{r}}_i)+\left(\frac{\lambda+1}{2\lambda+1}\right)^{1/2}\cdot\right.\right.$$
$$\left.\left.\cdot\, j_{\lambda-1}(qr_i)\underset{\sim}{Y}^{\mu}_{\lambda\lambda-1}(\hat{\underset{\sim}{r}}_i)\right]\frac{\mu_i}{2}\underset{\sim}{\sigma}(i)-j_\lambda(qr_i)\underset{\sim}{Y}^{\mu}_{\lambda\lambda1}(\hat{\underset{\sim}{r}}_i)\frac{e_i}{q}\underset{\sim}{\nabla}_{\underset{\sim}{r}_i}\right\} \tag{3.9}$$

and

$$T^E_{\lambda\mu}(q)=\sum_i\frac{\hbar}{Mc}q\left\{\left[-\left(\frac{\lambda}{2\lambda+1}\right)^{1/2}j_{\lambda+1}(qr_i)\underset{\sim}{Y}^{\mu}_{\lambda\lambda+1}(\hat{\underset{\sim}{r}}_i)+\left(\frac{\lambda+1}{2\lambda+1}\right)^{1/2}\cdot\right.\right.$$
$$\left.\left.\cdot\, j_{\lambda-1}(qr_i)\underset{\sim}{Y}^{\mu}_{\lambda\lambda-1}(\hat{\underset{\sim}{r}}_i)\right]\frac{e_i}{q}\underset{\sim}{\nabla}_{\underset{\sim}{r}_i}+j_\lambda(qr_i)\underset{\sim}{Y}^{\mu}_{\lambda\lambda1}(\hat{\underset{\sim}{r}}_i)\frac{\mu_i}{2}\underset{\sim}{\sigma}(i)\right\} \tag{3.10}$$

where M is the nucleon mass, $e_i=\frac{1}{2}(1+\tau_3(i))$, $\mu_i=\frac{1}{2}(1+\tau_3(i))\mu_p+\frac{1}{2}(1-\tau_3(i))\mu_n$, $\mu_p=2.79$, $\mu_n=-1.91$ and the Pauli spin and isospin operators of the i'th nucleon are $\underset{\sim}{\sigma}(i)$ and $\underset{\sim}{\tau}(i)$. The finite size effect of the proton can be taken into account multiplication by the appropriate proton form factor. The charge form factor of the proton may be approximated[47] by

$$\exp\left\{-a_p^2q^2/4\right\}\qquad a_p^2=0.43\,\mathrm{fm}^{-2} \tag{3.11}$$

By studying the low momentum transfer behaviour of the form factors further electromagnetic observables can be

deduced. In elastic scattering ($J_i = J_f = J$) the multipole expansion of the total charge form factor is given by

$$F_L^2(q^2) = F_{co}(q^2)^2 + \frac{1}{180}\left(\frac{Q^2 q^4}{Z^2}\right)\frac{1}{(2J+1)}\begin{pmatrix} J & 2 & J \\ -J & 0 & J \end{pmatrix}^2 + \cdots \qquad (3.12)$$

where $F_{co}(q^2)$ is the electric monopole form factor and Q is the electric quadrupole moment. For $q \to 0$, the monopole form factor may be expanded as

$$F_{co}(q^2)^2 = \left(1 - \frac{1}{6}\langle r^2\rangle q^2 + \frac{1}{120}\langle r^4\rangle q^4 + \cdots\right)^2 \qquad (3.13)$$

where $\langle r^2\rangle$ is the meansquare radius:

$$\langle r^2\rangle = -3\left.\frac{d^2 F_{co}}{dq^2}\right|_{q=0} \qquad (3.14)$$

From the behaviour of the transverse form factor in the long wave-length limit the ground state magnetic dipole moment can be obtained as

$$\mu^2 = 3\left(\frac{J}{J+1}\right)\left(\frac{Z M_c}{\hbar}\right)^2 \left.\frac{d^2 F_T^2}{dq^2}\right|_{q=0} \qquad (3.15)$$

where μ is expressed in units of nuclear magneton μ_N. In the long wave-length limit the reduced matrix element of the Coulomb multipole operator is related to the radiative decay lifetime τ_λ by

$$\tau_\lambda^{-1} = \frac{8\pi(\lambda+1)}{\lambda[(2\lambda+1)!!]^2}\frac{1}{\hbar}\left(\frac{E_\gamma}{\hbar c}\right)^{2\lambda+1} B(E\lambda, J_i \to J_f) \qquad (3.16)$$

where the reduced transition strength is

$$B(E\lambda, J_i \to J_f) = \frac{1}{2J_i+1}\left[\frac{(2\lambda+1)!!}{q^\lambda}\right]^2 \left|\langle J_f \| T_\lambda^c(q) \| J_i\rangle\right|^2 \qquad (3.17)$$

$q \to 0$

Following Oberall[48], the transition charge density is definied by

$$\rho_{if}^\lambda(r) = \langle J_f \| \rho_\lambda(r) \| J_i\rangle \qquad (3.18)$$

where

$$\rho_{\lambda\mu}(r) = \int d\hat{r}\; Y_{\lambda\mu}(\hat{r})\,\rho(\underset{\sim}{r}) \qquad (3.19)$$

The multipole component of the charge form factor can be expressed in terms of the transition charge density as

$$F_{c\lambda}(q) = \frac{(4\pi)^{1/2}}{Z(2J_i+1)^{1/2}}\int_0^\infty dr\; j_\lambda(qr)\,\rho_{if}^\lambda(r) \qquad (3.20)$$

Inversion of eq. (3.20) gives

$$\rho_{if}^\lambda(r) = \frac{Z(2J_i+1)^{1/2}}{\pi^{3/2}}\int_0^\infty dq\; j_\lambda(qr)\,F_{c\lambda}(q) \qquad (3.21)$$

3.2 Generator coordinate kernels of the electromagnetic multipole operators

To evaluate electromagnetic quantities in the framework of the GC method, we need the GC kernels of the electromagnetic multipole operators. In the following the calculation of the longitudinal form factor is sketched and the magnetic dipole form factor of the ground state is showed.

In the calculation of the charge form factor the centre-of-mass motion has to be treated correctly since, as it was shown[49,50], this motion may have a great influence on the charge form factor at high momentum transfer. Of course,

using the wave function (2.14) composed of the internal states (2.9), we do not face the problem of the centre-of-mass motion but a new difficulty arises. The calculation of the matrix elements of electromagnetic multipole operators in terms of internal wave functions, which are not Slater determinants, is very complicated. A way to overcome this difficulty is to keep all single particle coordinates but to use the wave function

$$\Psi_{\underset{\sim}{K}}(JM\alpha) = \frac{1}{(2\pi)^{3/2}} \exp\{i\underset{\sim}{K}\underset{\sim}{R}_{cm}\}\,\Psi^{int}(JM\alpha) \qquad (3.22)$$

The plane wave describing the centre-of-mass motion can be incorporated in the single particle orbits. The function $\Psi_{\underset{\sim}{K}}(JM\alpha)$ is then to be constructed from single particle orbits

$$\phi_{\underset{\sim}{K}}(\underset{\sim}{r}_i,\beta_i,\underset{\sim}{\xi}) = \frac{1}{(2\pi)^{3/2(A_\alpha+A_\alpha)}}\left(\frac{\beta}{\pi}\right)^{3/4} \exp\{i\underset{\sim}{K}\underset{\sim}{r}_i/(A_\alpha+A_\alpha) - \beta(\underset{\sim}{r}_i-\underset{\sim}{\xi})^2/2\} \qquad (3.23)$$

just as $\Psi(JM\alpha)$ is constructed from $\phi(\underset{\sim}{r}_i,\beta_i,\underset{\sim}{\xi})$ of (2.7). When the cluster width parameters are equal, the cumbersome linear momentum projection can be avoided by taking into account the Tassie-Barker correction[51] in the charge form factor.

With the definitions of section 2, the wave function (3.22) can be cast into the form

$$\Psi_{\underset{\sim}{K}}(JM\alpha) = \sum_{i=1}^{N_\alpha}\sum_{j=1}^{N_\alpha}\sum_{M_L M} \langle L M_L 1 M_\alpha | J M\rangle \int d\xi\, f_{ij}(J\alpha_\alpha,\xi) \int d\hat{\underset{\sim}{\xi}}\, Y_{LM_L}(\hat{\underset{\sim}{\xi}}) \int d\underset{\sim}{\zeta}\, \Psi_{\underset{\sim}{K}}(M_\alpha M_\alpha,\beta_i\beta_j,\underset{\sim}{\xi},\underset{\sim}{\zeta}) \qquad (3.24)$$

where

$$\Psi_{\underset{\sim}{K}}(M_\alpha M_\alpha,\beta_\alpha\beta_\alpha,\underset{\sim}{\xi}\,\underset{\sim}{\zeta}) = \mathcal{A}_{\alpha\alpha}\left(\prod_{i\in\alpha}\phi_{\underset{\sim}{K}}(\underset{\sim}{r}_i,\beta_\alpha,\underset{\sim}{\xi}_\alpha)\prod_{j\in\alpha}\phi_{\underset{\sim}{K}}(\underset{\sim}{r}_j,\beta_\alpha,\underset{\sim}{\xi}_\alpha)\sum_\alpha\sum_\alpha\right) \qquad (3.25)$$

The reduced matrix element of an irreducible tensor operator $O_{\lambda\mu}$ of rank λ between initial and final states of the form (3.24) can be written as

$$\langle\Psi_{\underset{\sim}{K}_f}(J_f\alpha_f)\|O_\lambda\|\Psi_{\underset{\sim}{K}_i}(J_i\alpha_i)\rangle = \sum_{i,i'=1}^{N_\alpha}\sum_{j,j'=1}^{N_\alpha}\int d\xi\, f_{ij}(J_f\alpha_f,\xi)^*\int d\xi'\, f_{i'j'}(J_i\alpha_i,\xi')\{O\}^{AMP}_{ij,i'j'}(\xi,\xi') \qquad (3.26)$$

where the angular momentum projected (AMP) kernel of $O_{\lambda\mu}$ is definied by

$$\{O\}^{AMP}_{ij,i'j'}(\xi,\xi') = \sum_{M_L M}\sum_{M'_L M'}(-)^{M_i-J_i}\langle\alpha_f M_f 1 M_L|J_f M_f\rangle\langle L_i M_i 1 M_L|J_i M_i\rangle \cdot \frac{1}{\langle J_i M_f J_i - M_i|\lambda\mu\rangle}\cdot\int d\hat{\underset{\sim}{\xi}}\, Y^*_{L_f M_f}(\hat{\underset{\sim}{\xi}})\int d\hat{\underset{\sim}{\xi}}'\, Y_{L_i M_i}(\hat{\underset{\sim}{\xi}}')\{O\}^{LMP}_{ij,i'j'}(\underset{\sim}{\xi},\underset{\sim}{\xi}') \qquad (3.27)$$

and the linear momentum projected kernel of $O_{\lambda\mu}$ is given in the form

$$\{O\}^{LMP}_{ij,i'j'}(\underset{\sim}{\xi},\underset{\sim}{\xi}') = \int d\underset{\sim}{\zeta}\int d\underset{\sim}{\zeta}'\langle\Psi_{\underset{\sim}{K}_f}(M_\alpha M_\alpha,\beta_\alpha\beta_\alpha,\underset{\sim}{\xi}\,\underset{\sim}{\zeta})|O_{\lambda\mu}|\Psi_{\underset{\sim}{K}_i}(M_\alpha M_\alpha,\beta_\alpha\beta_\alpha,\underset{\sim}{\xi}'\,\underset{\sim}{\zeta}')\rangle \qquad (3.28)$$

where $\hat{\underset{\sim}{\xi}}$ and $\hat{\underset{\sim}{\xi}}'$ denote the angle variables of the vectors $\underset{\sim}{\xi}$ and $\underset{\sim}{\xi}'$. The integrand of Eq. (3.28) can be calculated straightforwardly due to the fact that the wave functions appearing in it are simple Slater determinants.

Because of computational convenience, the Coulomb multipole operator given in Eq. (3.8) was rewritten in the form

$$T^c_{\lambda\mu}(q) = \sum_k e_k \frac{1}{4\pi\, c^\lambda} \int d\hat{q}\; Y_{\lambda\mu}(\hat{q}) \exp\{i q r_k\} \qquad (3.29)$$

In the following the wave function (3.24) is assumed to be normalized i.e. $\langle \Psi_{K_f}(J_f M_f \alpha_f) | \Psi_{K_i}(J_i M_i \alpha_i)\rangle = \delta(K_i - K_f)$ and from the GC kernels the Dirac-delta function $\delta(K_i - q - K_f)$ expressing the conservation of the total linear momentum will be omitted.

A lengthy but straightforward calculation gives the linear momentum projected kernel of $T^c_{\lambda\mu}(q)$:

$$\left\{T^c_{\lambda\mu}(q)\right\}^{LMP}_{\alpha_j\alpha_i^{J_i}}(\beta,\beta') = \sum_{k=1}^{6}\sum_{\varepsilon} (-)^\varepsilon M_\varepsilon \exp\{-b_{\varepsilon,k}\beta_j^2 - u_\varepsilon \beta^2 - u'_\varepsilon \beta'^2\} \frac{e_k}{4\pi c^\lambda} \cdot \Delta_\varepsilon \cdot \int d\hat{q}\; Y_{\lambda\mu}(\hat{q})\; \exp\{i f_{\varepsilon,k} q \beta + i f'_{\varepsilon,k} q \beta'\} \qquad (3.30)$$

where

$$\Delta_\varepsilon = \delta_{\tau_1\sigma_3(\varepsilon_1)} \cdots \delta_{\tau_j\sigma_3(\varepsilon_6)} \cdot \delta_{\tau_1\tau_3(\varepsilon_1)} \cdots \delta_{\tau_j\tau_3(\varepsilon_6)} \qquad (3.31)$$

originates from the inner products of the spin and isospin functions, $\sigma_{3(i)}$ and $\tau_{3(i)}$ are the third component of the spin and isospin of the i'th nucleon and δ_{ij} is the Kronecker symbol. The summations in Eq. (3.30) run over the indexes of the nucleons and permutations. The coefficients M_ε, $b_{\varepsilon,k}$, u_ε, ... still depend on the cluster width parameters $\beta^i_\alpha, \beta^j_\alpha$ and $\beta^{i'}_\alpha$. Out of 6·6! terms of the sum in (3.30) only four different ones survive. The terms in (3.30) may be

classified according to how many particles are exchanged between α and α and the manner how the photon interacts with a particular nucleon in the clusters.[52] Explicit expressions of the coefficients M_ε, $b_{\varepsilon,k}$, u_ε, ... will be published elsewhere. Expanding the exponential function in (3.30) into spherical harmonics of the angles $\hat{\beta}$ and $\hat{\beta}'$ the integration indicated in Eq. (3.27) can easily be carried out, and after some angular momentum algebraic manipulation the AMP kernel of $T^c_{\lambda\mu}(q)$ can be written in the form

$$\left\{T^c_\lambda(q)\right\}^{AMP}_{\alpha_j\alpha_i^{J_i}} = (4\pi)^{1/2} \hat{J}_i \hat{J}_f \hat{\lambda} \sum_\varepsilon \sum_{k=1}^{6} \sum_{L_1L'L''=0}^{\infty} i^{L+L'+\lambda} \hat{L}^2 \hat{L}'^2 \hat{L}''^2 (-)^{L'+\lambda} \cdot \begin{pmatrix} \lambda & L & L'' \\ 0 & 0 & 0 \end{pmatrix} \begin{pmatrix} J_f & L & L'' \\ 0 & 0 & 0 \end{pmatrix} \begin{pmatrix} J_i & L' & L'' \\ 0 & 0 & 0 \end{pmatrix} \begin{Bmatrix} J_f & \lambda & J_i \\ L' & L'' & L \end{Bmatrix} j_L(f_{\varepsilon,k} q \beta) j_{L'}(f'_{\varepsilon,k} q \beta') \cdot i_L(W_\varepsilon \beta\beta') \exp\{-b_{\varepsilon,k} q^2 - u_\varepsilon \beta^2 - u'_\varepsilon \beta'^2\} \cdot (-)^\varepsilon M_\varepsilon \cdot \Delta_\varepsilon \cdot e_k \qquad (3.32)$$

where i_L is the modified spherical harmonics of the first kind and $\hat{L} = (2L+1)^{1/2}$.

For elastic scattering $J_i = J_f = 1$ and $\alpha_i = \alpha_f = 0$ the expression (3.32) becomes simpler. Using Eq. (3.3) the AMP kernel of the Coulomb monopole form factor emerges as

$$\left\{F_{c0}(q^2)\right\}^{AMP}_{\alpha_j\alpha_i^{J_i}} = \left(\frac{4\pi}{3}\right)^2 \left| \sum_\varepsilon \sum_{k=1}^{6} \sum_{L=0}^{\infty} (-)^\varepsilon M_\varepsilon (-)^L (2L+1) \cdot j_L(f_{\varepsilon,k} q \beta) \cdot j_L(f'_{\varepsilon,k} q \beta') \cdot i_L(W_\varepsilon \beta\beta') \exp\{-b_{\varepsilon,k} q^2 - u_\varepsilon \beta^2 - u'_\varepsilon \beta'^2\} \cdot e_k \Delta_\varepsilon \right|^2 \qquad (3.33)$$

The AMP kernel of the mean square radius can be derived combining Eqs. (3.14) and (3.33):

$$\left\{\langle\tau^2\rangle\right\}^{AMP}_{i_f j_f i_i j_i}(s,s') = -4\pi \sum_{\varepsilon}\sum_{k=1}^{6} (-)^{\varepsilon} M_{\varepsilon} \exp\{-u_{\varepsilon} s^2 - u'_{\varepsilon} s'^2\} \cdot e_k \Delta_{\varepsilon} \cdot [$$

$$i_0(W_{\varepsilon} s s') \left(2 b_{\varepsilon i k} - \frac{1}{3} f^2_{\varepsilon i k} s^2 - \frac{1}{3} f'^2_{\varepsilon i k} s'^2\right) - \frac{2}{3} i_1(W_{\varepsilon} s s') f_{\varepsilon i k} f'_{\varepsilon i k} s s'] \quad . \tag{3.34}$$

According to Eq. (3.21) the charge density of the ground state is the Fourier transform of the charge form factor F_{c0}. This transformation was done numerically in the actual calculation.

The charge form factor F^*_{c2} of the inelastic electron scattering leading to the first excited state of ^{6}Li can be obtained from the general results (3.32) and (3.3) by putting the corresponding quantum numbers into these expressions. In our model the quantum numbers $\mathcal{L}=0$ and $\mathcal{L}=2$ are assigned to the ground and first excited states of ^{6}Li. The AMP kernel of $F^*_{c2}(q)^2$ reads

$$\left\{F^*_{c2}(q)^2\right\}^{AMP}_{i_f j_f i_i j_i}(s,s') = \frac{112\pi^2}{27} \left| \sum_{\varepsilon}\sum_{k=1}^{6}\sum_{L=0}^{\infty} \sum_{L'=|L-2|}^{L+2} (-)^{\varepsilon} M_{\varepsilon} e_k i^{L+L'} \cdot \Delta_{\varepsilon} \right.$$

$$\left. \hat{L}^2 \hat{L}'^2 \begin{pmatrix} 2 & L & L' \\ 0 & 0 & 0 \end{pmatrix}^2 \exp\{-b_{\varepsilon i k} q^2 - u_{\varepsilon} s^2 - u'_{\varepsilon} s'^2\} j_L(f_{\varepsilon i k} q s) j_{L'}(f'_{\varepsilon i k} q s') i_{L'}(W_{\varepsilon} s s') \right|^2 \tag{3.35}$$

Substituting the expression (3.35) into the Eq. (3.17) and taking the limit $q \to 0$, we obtain the general formula of the electric 2^2 pole reduced transition strength

$$\left\{B(E\lambda, J_i \to J_f)\right\}^{AMP}_{i_f j_f i_i j_i}(s,s') = J_f^2 \left[(2\lambda+1)!!\right]^2 \hat{L}_i^2 \hat{L}_f^2 \hat{\lambda}^2 \begin{Bmatrix} L_f & J_f & I \\ J_i & L_i & \lambda \end{Bmatrix} (-)^{2(J_f+1)} \cdot \left(\frac{e}{4\pi}\right)^2 \cdot$$

$$\left| \sum_{\varepsilon}\sum_{k=1}^{6} \sum_{L_i L'_i L''=0}^{\infty} (-)^{\varepsilon} M_{\varepsilon} i^{L_i+L'_i+\lambda} (-)^{L'_i+\lambda} \delta_{L_i+L'_i,2} \hat{L}_i^2 \hat{L}'^2_i \hat{L}''^2 \exp\{-u_{\varepsilon} s^2 - u'_{\varepsilon} s'^2\} e_k \Delta_{\varepsilon} \right. \tag{3.36}$$

$$\left. i_{L''}(W_{\varepsilon} s s') (f_{\varepsilon i k} s)^{L_i} (f'_{\varepsilon i k} s')^{L'_i} \begin{pmatrix} \lambda & L_i & L'_i \\ 0 & 0 & 0 \end{pmatrix} \begin{pmatrix} L_f & L'_i & L'' \\ 0 & 0 & 0 \end{pmatrix} \begin{pmatrix} L_i & L'_i & L'' \\ 0 & 0 & 0 \end{pmatrix} \begin{Bmatrix} L_f & \lambda & L_i \\ L'' & L & L'_i \end{Bmatrix} \cdot \left((2L+1)!! (2L'+1)!!\right)^{-1} \right|^2$$

The specialization of the expression (3.36) for the transition $3^+ \to 1^+$ leads to the form

$$2\pi 0\, \pi \left| \sum_{\varepsilon}\sum_{k=1}^{6}\sum_{L L' =0}^{\infty} i^{L+L'} \delta_{L+L',2} \hat{L}^2 \hat{L}'^2 (-)^{\varepsilon} M_{\varepsilon} \exp\{-u_{\varepsilon} s^2 - u'_{\varepsilon} s'^2\} i_{L'}(W_{\varepsilon} s s') \cdot \right.$$

$$\left. e_k \Delta_{\varepsilon} \cdot \begin{pmatrix} 2 & L & L' \\ 0 & 0 & 0 \end{pmatrix}^2 (f_{\varepsilon i k} s)^L (f'_{\varepsilon i k} s')^{L'} \left((2L+1)!! (2L'+1)!!\right)^{-1} \right|^2 \tag{3.37}$$

We note by passing that the equations (3.32) and (3.36) are not restricted to ^{6}Li. They are generally valid for any two s-wave cluster nucleus provided the summation over k and ε run over the nucleons and permutations involved by the particular nucleus. General expressions for the coefficients $M_{\varepsilon}, b_{\varepsilon i k}, u_{\varepsilon}, \ldots$ can also be given. They depend on the mass number of the clusters and, of course on the cluster width parameters.

After similar steps, the transverse magnetic dipole form factor F_{M1} of the ground state can be cast into the form

$$\left\{F_{M1}(q)^2\right\}^{AMP}_{i_f j_f i_i j_i}(s,s') = \frac{64\pi^2}{27} \left(\frac{\hbar}{Mc}\right)^2 q^2 \left| \sum_{\varepsilon}\sum_{k=1}^{6}\sum_{L=0}^{\infty} (-)^{\varepsilon} (-)^L \hat{L}^2 M_{\varepsilon} u_k \sigma_k \cdot \right.$$

$$\left. j_L(f_{\varepsilon i k} q s) j_L(f'_{\varepsilon i k} q s') i_L(W_{\varepsilon} s s') \cdot \exp\{-b_{\varepsilon i k} q^2 - u_{\varepsilon} s^2 - u'_{\varepsilon} s'^2\} \cdot \Delta_{\varepsilon} \right|^2 \tag{3.38}$$

where σ_k is 1/2 for spin-up and -1/2 for spin-down states of the k'th nucleon. It is worthwhile to mention that in the present model of ^{6}Li the convection current part of the current density operator happens to give vanishing contribution to F_{M1}. After taking into account Eqs. (3.38) and (3.15) it turns out that the GC kernel of the ground state magnetic dipole moment μ is proportional to the norm kernel

$$\{\mu\}^{AMP}_{i_j i'_j j}(s,s') = (\mu_p+\mu_n)\, N^{AMP}_{i_j i'_j j}(s,s') \qquad (3.39)$$

where the norm kernel of the ground state is given by

$$N^{AMP}_{i_j i'_j j}(s,s') = 4\pi \sum_{\xi} (-)^{\xi} M_\xi \exp\{-u_\xi s^2 - u'_\xi s'^2\} i_o(w_\xi ss') \cdot \Delta_\xi \qquad (3.40)$$

The coefficients u_ξ, u'_ξ, w_ξ, and M_ξ in Eq. (3.30) are identical to those involved in the norm kernel (3.40). The consequence of Eq. (3.39) is that the magnetic dipole moment of the ground state, independent of the model and NN interaction used, is $\mu = 0.88$ nuclear magneton.

4. Results

4.1 Description of the free clusters

For the description of the ground state and breathing excited states of the free clusters the intrinsic wave functions of the form (2.19) were used. In the MW model, to get a rough energy convergence within 1-2 keV, it was enough to use three and five width parameters for α and d respectively. They were determined by minimizing the microscopic cluster hamiltonian. The optimum values of the widths are shown in Table 1 for the different models and interactions used.

In Table 2 the calculated and experimental values of the binding energies and root mean square (rms) radii of

the clusters are displayed. The interactions V2 and BB1 are better for α than for d and, on the contrary, the MN force gives a good description for d but fails for α. The rms radius of d is strikingly large in the MW model using the V2 or BB1 force. Direct numerical integrations of the Schrödinger equation of the deuteron, using the computer code GAMOW[55], give virtually the same results as presented in Table 2 (e.g. the binding energies are -0.6083, -1.0173 and -2.2018 MeV for V2, BB1 and MN forces). Thus the MW model of d is essentially exact and adequate to the interactions used.

The ground state charge form factor of a nucleus with mass number less than five, assuming a normalized wave function of the form (2.19), may be written in the following form

$$|F_L(q^2)|^2 = 4\pi \left| \sum_{i_j=1}^{N_c} \left(f_c^{i_j,1}\right)^* f_c^{j,1} \left[\frac{2\pi\,(\beta_c^{i*}+\beta_c^{j})}{A_c\,\beta_c^{i*}\beta_c^{j}}\right]^{3/2} \cdot \left[\frac{4\beta_c^{i*}\beta_c^{j}}{(\beta_c^{i*}+\beta_c^{j})^2}\right]^{3A_c/4} \cdot \exp\left\{-q^2\,(A_c-1)/\left(2A_c(\beta_c^{i*}+\beta_c^{j})\right)\right\}\right|^2 \qquad (4.1)$$

In Figure 1 the measured values and some calculated elastic charge form factors of the α particle are show as functions of the squared momentum transfer q^2. In a single-width model the charge form factor depends only on the width parameter (independently of the interaction) and according to the expression (4.1), a diffraction dip cannot develop. In the MW model the calculated diffraction minima appear around

q^2=24.05, 16.25 and 23.45 fm^{-2} with the V2,BBl and MN interaction, respectively. The failure of the simple shell-model type description to reproduce the diffraction dip is well known and it has been shown that the short range correlation[9,57] of the nucleons and meson exchange currents[58,59] play substantial roles in the region of the minimum and the secondary maximum. In the small momentum transfer (SMT) region (q^2< 8 fm^{-2}) the best agreements with experiment were obtained using by the BBl force. In spite of the fact that the rms radius of α is quite good with the MN interaction, the discrepancy in the binding energy appears also in the shape of the calculated charge form factor. In the MW model the charge form factor of α changes, with respect to the single width models, only very slightly in the SMT region.

For practical reasons the elastic electron-deuteron scattering cross section is usually given in the form[60]

$$\sigma(\theta) = \frac{\sigma_M}{1+\frac{2E}{Mc^2}\sin^2\theta/2}\left[A(q^2)+\tfrac{1}{2}q^2\theta/2 \cdot B(q^2)\right] \qquad (4.2)$$

where the invariant structure function $A(q^2)$ is composed of the longitudinal monopole (F_{C0}), quadrupole (F_{C2}) and transverse dipole magnetic (F_{M1}) form factors and $B(q^2)$ is proportional to F_{M1}. In our model it can be shown that

$$A(q^2) = C_E(q^2)^2 \cdot \left[1+\frac{2}{3}\eta(1+\eta)\frac{M_d^2}{M^2}(\mu_p+\mu_n)^2\right] \qquad (4.3)$$

and

$$B(q^2) = C_E(q^2)^2 \cdot \frac{4}{3}\eta(1+\eta)\frac{M_d^2}{M^2}(\mu_p+\mu_n)^2 \qquad (4.4)$$

where $\eta = \hbar^2 q^2/4M_d^2c^2$ and

$$C_E(q^2)^2 = \left|\sum_{s=1}^{N_d}\sum_{j=1}^{N_d}\left(f_d^{s,l}\right)^* f_d^{j,l}\cdot\left[\frac{4\pi}{(\beta_d^s+\beta_d^j)}\right]^{3/2}\cdot\exp\left\{-q^2/4(\beta_d^s+\beta_d^j)\right\}\right|^2 \qquad (4.5)$$

In Figures 2 and 3 the experimental values and the calculated curves of the invariant structure functions $A(q^2)$ and $B(q^2)$ are displayed. Using the MN interaction the MW model gives a very good description of the structure function $A(q^2)$ and reproduces $B(q^2)$ satisfactorily in the SMT region. With the BBl and V2 interactions, on the contrary, the curves of the MW model decrease too rapidly, and the agreement with experiment is bad. In the single width models the better accord must be accidental since MW is a better approximation. At momentum transfers larger than 8 fm^{-2} even our best model fails to agree with experiment. The reason is that in this region the quadrupole component of $A(q^2)$ becomes dominant,[61] and, due to the lack of the tensor force, the F_{C2} contribution is missing to $A(q^2)$ in our model. For a better agreement at higher q^2 values it seems inevitable to take into account meson exchange currents and relativistic corrections.[67]

4.2 Electromagnetic properties of ^{6}Li in a cluster model with breathing clusters

A. Bulk properties

For the discrete values of the width parameters in the cluster model with breathing clusters we adopted the values that are optimal in the problems of the free clusters (Table 1). The generator coordinate s was also discretized and the selected 11 points were equidistantly distributed in the interval (1 fm, 11 fm).

In the calculation of the ground state of ^{6}Li one exchange parameter of each interaction was adjusted (see Table 3.) so as to give the correct αd threshold energy (1.47 MeV). The fact that the energies of the α and d particles depend only on the combinations $W-M$ and $W+M+B+H$ gives us the chance of modifying the interactions without changing the properties of the free clusters. The reason for the adjustment is that the electromagnetic properties are sensitive to the long range part of the wave function, which depends strongly on the threshold energy. The fact that the separation energy is correct in each model makes possible a consistent comparision between different interactions and models.

In Table 4 some calculated bulk properties of ^{6}Li are compared with the experimental values. Since in the case of each interaction and model the alpha and deuteron

separation energies are correct the quantitative differences in the binding energy of ^{6}Li derive from the ground state energies of the free clusters. A comparison between the models CW and MW with the same interaction can be found in ref.[17] In the model D_2D_2 the calculated rms radii of the ground state agree with the experimental value within the error of the measurement for each interaction. It shows the stability of the α particle that the switching off of the distortion of α changes the rms radius of ^{6}Li by at most 0.02 fm. On the contrary, the neglect of the distortion of d causes a considerable increase in the rms radius in the case of the V2 and BBl interactions. The rms radius proves to be stable as regards cluster distortions provided the MN force is used.

The calculated magnetic dipole moment of the ground state $0.88\mu_N$, which is model- and interaction-independent in our framework, compares satisfactorily with the experimental value $0.82\mu_N$.

The wave function of the first excited state of ^{6}Li is also assumed to have the form (2.14) and the same set of GC's was used as in the description of the ground state but now the relative orbital angular momentum between the clusters is taken to be 2 instead of 0. First the same interactions were considered as in the calculation of the ground state. However, the effective forces applied do not contain

spin-orbit terms and it is expected that the energy of the first excited state predicted by these models correspond to the weighted average of the excitation energies of the first triplet 1^+, 2^+ and 3^+ states of ^{6}Li. Since the inelastic electron scattering and γ decay rate are sensitive to the excitation energy the nucleon-nucleon interactions of Table 3. were readjusted so as to reproduce the correct excitation energy. Two remarks concerning this readjustment should be made. Firstly, this procedure might be considered as the simulation of the neglected spin-orbit force, and, secondly, due to the angular parts of the relative wave functions, the orthogonality of the ground and excited states is still held.

With the model $G_\alpha G_d$ excepted, the results concerning the excitation energy of the first excited 3^+ state of ^{6}Li and the reduced transition strength $B(E2, 3^+ \to 1^+)$, were obtained in fair agreement with experiment. Our results show that the α -cluster remains stable but the deuteron is strongly distorted in the first excited state as well.

B. Electromagnetic form factors

The ground state charge form factors, calculated with different models and interactions, are displayed in Figures 4 and 5. The following features can be observed. In the models CW the characteristic diffraction dip always appears but two defects can be seen: first, the diffraction dip is

not at the right position and, second, even in the SMT region there is no quantitative agreement with the experiment. We see that the best result is achieved by the MN force, however, the choice of one common width parameter of the clusters is quite arbitrary, and a small change in the width parameter destroys the good agreement in the SMT region.

In the models DW the diffraction dip disappears but at the same time in the SMT region the agreement with the experiment is greatly improved. The diffraction dip disappears also in the shell model description[50] when the width parameters of the s- and p-wave orbits are chosen to be different in a particular way. Of course, in a phenomenological cluster model the different widths of the clusters can be chosen so as to obtain a good description of $|F_{CO}|^2$ including the diffraction dip. However a fitting of the width parameters of the clusters to the form factor F_{CO} leads to the result[31] that the cluster d is more extended inside ^{6}Li than the free deuteron. This is contrary, to the results of the dynamical calculations, which predict the shrinking of the deuteron[14,17,23,7] and thus seems unphysical. We have adopted the viewpoint of the dynamical cluster models, and want to carry it through with all its implications.

The $D_\alpha D_d$ model can record a remarkable success by reproducing $|F_{CO}|^2$ in the SMT region. In the following we shell give account of the tests to establish the cause of

its failure to reproduce the diffraction dip.

We tested the forces against another one, which was optimized to our $D_\alpha D_d$ model.[72] This force gives virtually exact binding energies and rms radii for the nuclei ^2H, ^3H, ^3He and ^4He, reproduces the experimental binding energy of ^6Li and, in addition, it predicts the binding energies of the other nuclei of two s-wave clusters, viz. ^5He, ^5Li, ^7Li, ^7Be, and ^8Be with an accuracy of 1 MeV. This force produced no diffraction dip of $|F_{co}|^2$ either.

It was observed that using fewer cluster width parameters, for example one for α and two for d as in Ref. 23, the diffraction dip reappears. The position of the diffraction minimum is very sensitive to the values of the widths. Using the interaction and width parameters given in Ref. 23 the minimum is obtained around 8.5 fm^{-2} but when the cluster stability condition is imposed the dip is shifted to a considerably higher q^2 value (11.3 fm^{-2}). However, as we have seen, a proper description of α and d requires more width parameters, and a corresponding extension of the model space for ^6Li invariably causes the diffraction minimum to disappear.

A qualitative analysis of the form factor may be implemented by neglecting the intercluster antisymmetrization. In this approximation F_{co} reduces to

$$F_{co}(q) = \frac{2}{3} F_{\alpha d}\left(\tfrac{1}{3}q\right) F_\alpha(q) + \frac{1}{3} F_{\alpha d}\left(\tfrac{2}{3}q\right) F_d(q) \qquad (4.6)$$

where $F_\alpha(q)$ and $F_d(q)$ are the charge form factors of the clusters α and d, respectively, and $F_{\alpha d}(q)$ is the Fourier transform of the wave function of the relative motion of the clusters. In our models the presence of the diffraction dip may be explained in the following way. The wave function of the relative motion that can be used in a non-anti-symmetrized model looks like a 2s-type harmonic oscillator wave function. The Fourier transform of a relative function of this type has both positive and negative parts. In the models CW, DW and $G_\alpha G_d$ the possible diffraction dip of $|F_{co}(q)|^2$ can only be attributed to the relative motion since, on the one hand, according to Eq. (4.1), the form factors of the clusters are positive everywhere when each cluster is described by one width parameter, and, on the other hand in the MW model of α and d the sign change in the form factors $F_\alpha(q)$ and $F_d(q)$ are at q^2 values much higher than the minimum of the squared form factor of ^6Li.
This picture becomes more complicated in the models $D_\alpha D_d$ $G_\alpha G_d$ and $D_\alpha G_d$ because of an interference with the form factors of the cluster excited states. The effect of these extra terms may be interpreted by saying that the dip due to the relative motion is shifted away and due to the separate clusters are not brought down sufficiently for ^6Li.
Thus the diffraction dip of ^6Li can be derived neither from those present in the models of the separate clusters

nor from that of the relative motion. However, tha actual experimental $|F_{c0}(q)|^2$ of the α-particle does contain a diffraction dip almost coinciding with that of ^{6}Li. Our analysis thus strongly indicates that the latter could only be derived from the former. It has been proposed that the diffraction minimum of the form factor of α can only be explained by introducing Jastrow-correlation into the wave function. Thus our conclusion is that in the understanding of the ground state charge form factor of ^{6}Li the short range NN correlation must play a substantial role. Our study of the αd fragmentation strength also points to some missing short range correlation.[72]

However, careful analyses have to be carried out since the region of the dip of the squared charge form factor of ^{6}Li is just the momentum transfer area where the non-nucleonic degrees of freedom come in to play. E.g. the meson exchange currents may help to explain the second maximum of the squared form factor of ^{6}Li.[73]

Now let us turn to the study of the cluster distortions. In Figure 5 the calculated charge form factor of the models $D_\alpha D_d$, $G_\alpha D_d$ and $G_\alpha G_d$ are shown. Both the alpha and deuteron distortions have an effect on the shape of the charge form factor only at high momentum transfer region ($q^2 > 8$ fm^{-2}) but the former to a lesser extent.

Our results show that the good agreement with experiment in the SMT region is in consequence of using realistic

ground states of the clusters.

The calculated charge density $\rho(r)$ of the ground state is shown in Figures 7 and 8 together with the experimentally fitted charge density distribution of Li et al.[70] that contains six adjustable parameters. Using the model CW the calculated curves of $\rho(r)$ deviat badly from the fitted one. The charge density of the central region is considerably underestimated with the forces V2 and BB1 and is overshot with the MN interaction. Whichever interaction is used, the distortion enhances the charge density at the vicinity of the origin. With the model $D_\alpha D_d$ used, the calculated charge densities are close to the phenomenological one when interactions V2 or BB1 are used but the value remains too large at the centre in the case of the force MN. It was observed in cluster and shell model studies that short range NN correlations through a Jastrow function depress the charge density around the centre but enhance it in the region between 2 and 4 fm.[7,9,33] These are the very areas where our calculated charge densities are not in agreement with the experimentally fitted curve. Thus it may be hoped that with Jastrow correlation the high momentum behaviour of the charge form factor of the cluster model with breathing clusters can also be improved.

The calculated squared inelastic charge form factor $|F^*_{C2}(q)|^2$ of the excitation of the 2.18 MeV state is presented in Figures 8 and 9. The results of the model CW

in each case are in quite good agreement with the experimental data. Although the introduction of different width parameters for the clusters makes the results worse, especially after the maximum of the squared form factor $|F_{C2}^{*}|^2$, but the inelastic charge form factor of the model $D_\alpha D_d$ reproduces the measured values very well. It is remarkable that here the maximum in $|F_{C2}^{*}|^2$, usually described unsatisfactorily[11,78], is predicted in good agreement with experiment.

The stability of the α cluster is nicely demonstrated in the model calculations $G_\alpha D_d$, in Fig. 9 the difference between the curves of $|F_{C2}^{*}|^2$ calculated with the models $D_\alpha D_d$ and $G_\alpha G_d$ is unobservable in the case of each interaction. According to the calculation with the model $G_\alpha G_d$ the distortion of the d-cluster greatly influences the shape of the squared inelastic charge form factor even at very small momentum transfer. For magnetic form factor of the ground state of ^{6}Li our calculation is the first in a dynamical microscopic cluster model. Our calculated elastic transverse form factor of ^{6}Li and the measured data are depicted in Figures 10 and 11. The rough shape of the magnetic dipole form factor $|F_{M1}|^2$ is reproduced by each model and interaction considered. Using the force V2 or BB1 the diffraction minimum of $|F_{M1}|^2$ was predicted at too small momentum transfer and after the first maximum of $|F_{M1}|^2$ the calculated curves deviate significantly from the

measured values. However, the interaction MN produces nice agreement with experiment in the whole region of the measured momentum transfer. The good result gained with the MN force may be attributed to the proper description of the deuteron since the magnetic form factor of ^{6}Li depends mainly on the nucleons of the deuteron cluster. The effect of the breathing excited states of α on the form factor $|F_{M1}|^2$ is almost unobservable in Figure 11. The breathing states of d, on the contrary, markedly influence the behaviour of $|F_{M1}|^2$ around its second maximum and shift the place of the minimum of $|F_{M1}|^2$.

Simultaneous description of the longitudinal and transverse form factors of ^{6}Li has been successful neither in terms of three-body model[16] nor standard phenomenological cluster models.[31,32] Our results show that using dynamically determined wave functions in a microscopic cluster model with breathing clusters and a realistic interaction, all form factors F_{C0}, F_{M1} and F_{C1}^{*} can be obtained with good accuracy in the SMT region.

Summary

The effect of the breathing excited states of the deuteron and the alpha cluster on the electromagnetic properties of ^{6}Li was examined using a GC-type cluster model of ^{6}Li. It should be underlined that the calculations are free from the spurious centre-of-mass motion and arbitrary parameters.

The oscillator width parameters of the clusters and the exchange mixtures of the NN interaction were determined by the cluster stability condition and by the correct separation energy value, respectively. In order to see the force dependence the calculations were carried out with three different central interactions. The following conclusions are found to be general, independent of the force.

It was found that at low momentum transfer ($q^2 < 8 fm^{-2}$) the charge form factor of the ground state of ^6Li was modified very slightly by mixing the breathing excited states of the clusters into the wave function. What is important in the low-q^2 region is the quality of the ground states of the clusters. With a realistic ground state of the deuteron, the monopole charge form factor of ^6Li is reproduced excelently in the low-q^2 region. On the other hand, around and beyond the diffraction dip the shape of the squared charge form factor is greatly influenced by the breathing excited states of the deuteron.

An unexpected by-product of the increase of the model space by including more and more breathing excited states of the clusters into the wave function is the gradual disappearance of the experimentally observed diffraction minimum of the squared charge form factor $|F_{C0}(q)|^2$. As the extension of the model space is bound to improve the wave function for a fixed Hamiltonian, this deficiency most

probably reflects the important role played by the neglected non-nucleonic degrees of freedom in this momentum transfer region. These non-nucleonic degrees of freedom manifest themselves partly in the repulsive core of the effective NN interaction. However, our effective NN interactions contain only repulsive cores of modest strength. It would be desirable to use more saturating NN interactions but in that case Jastrow correlation functions are to be used. At any rate, the short range NN correlation was shown to be very important in the explanation of the diffraction dip of ^6Li in shell model description[6,7,9,73] as well. To get quantitative agreement in the high momentum transfer region other effects also have to be taken into account explicitly, e.g. the usual underestimation of the second maximum of the squared charge form factor can be partly remedied by considering meson exchange currents.

The transverse form factor of the ground state of ^6Li was not studied earlier with dynamical microscopic cluster models. Our results showed that the magnetic dipole- and charge- form factors of the ground state can be well described simultaneously using the same variationally determined wave function. The rough shape of the magnetic form factor was reproduced with each model and interaction used. However good agreement in the whole experimentally measured region was only reached by using an interaction which describes

properly the deuteron (e.g. the Minnesota force). The excited states of the cluster d effect the position of the diffraction minimum of $|F_{M1}(q)|^2$ and its shape around the second maximum.

The influence of the breathing excited states of d on the squared inelastic charge quadrupole form factor $|F^*_{C2}(q)|^2$ is shown to be very important. The shape of the squared form factor $|F^*_{C2}(q)|^2$ below and around its first maximum is reproduced only with the inclusion of the breating excited states of d. The predicted curve of $|F^*_{C2}(q)|^2$ is in very good agreement with the measurement. The effect of the excited states of d on $|F^*_{C2}(q)|^2$ is larger than on $|F_{C0}(q)|^2$; it is considerable even in the low-q^2 region. This can be explained by assuming it is more probable to find excited d configurations in an excited state than in the ground state of ^{6}Li.

The stability of the α particle was demonstrated in a number of cluster model calculations for α scattering. Our results also indicate the rigidity of the α -cluster. In the calculations of the form factors $|F_{C0}|^2$, $|F_{M1}|^2$ and $|F^*_{C2}|^2$ the breathing excited states of α can be neglected at least at small momentum transfer but even the distortion of the cluster α can be observed in the high q^2 region.

All in all, the cluster model with breathing clusters was shown to be able to give a very good simultaneous description of the elastic and inelastic charge form factors and the

elastic magnetic form factor in the low-q^2 region. However, in order to clarify the discrepancy found in the high momentum behaviour of the form factor $|F_{C0}|^2$ and to describe the quadrupole moment of the ground state our model has to be improved in two respects: first, the flexibility of the wave function has to be increased by employing correlation function of the Jastrow type to reckon with the short range NN correlation, and, second, the central NN interaction has to be replaced by a more realistic one containing spin-orbit and tensor components.

Aknowledgments

A.T.K. wishes to thank Prof. G. Schatz and the Kernforschungszentrum Karlsruhe for their kind hospitality Prof. A. Faessler and Dr. R. G. Lovas for useful discussions. A.T.K. is indebted to Prof. R. Neuhausen for providing him with the magnetic form factor data of Dr. L. Lapikás.

References

+ Deceased.

[1] G.R. Burleson and R. Hofstadter, Phys.Rev. 112,1282(1958).

[2] L.R.B. Elton, Nuclear Sizes (Oxford University Press, 1961).

[3] D.F. Jackson, Proc. Phys. Soc. 76,949(1960).

[4] M.A.K. Lodhi, Nucl.Phys. 80,125(1966).

[5] L.R.B. Elton and M.A.K. Lodhi, Nucl.Phys. 66,209(1965).

[6] S.S.M. Wong and D.L. Lin, Nucl.Phys. A101,663(1967).

[7] C. Ciofi degli Atti and N.M. Kabachnik, Phys. Rev. C1, 809 (1970).

[8] D.A. Sparrow and W.J. Gerace, Nucl.Phys. A145, 289 (1969).

[9] C. Ciofi degli Atti, Nucl.Phys. A129, 350 (1969).

[10] M.A.K. Lodhi, Phys. Rev. C3, 503 (1971).

[11] G.L. Payne and B.P. Nigam, Phys. Rev. C21, 1177 (1979).

[12] K. Wildermuth and Y.C. Tang, A Unified Theory of the Nucleus (Academic Press New York, 1977).

[13] R. Krivec and M.V. Mihailovic, J. Phys. G: Nucl. Phys. 8, 821 (1982).

[14] R. Beck, F. Dickmann and R.G. Lovas, Ann. Phys. in press.

[15] J. Bang and C. Gignoux, Nucl. Phys. A313, 119 (1979).

[16] V.I. Kukulin, V.M. Krasnopol'sky, V.T. Voronchev, and P.B. Sazanov. Nucl. Phys. A417, 128 (1984).

[17] R. Beck, F. Dickmann and A.T. Kruppa, Phys. Rev. C30, 1044 (1984).

[18] D.R. Thompson and Y.C. Tang, Phys. Rev. 179, 971 (1969).

[19] H. Jacobs, K. Wildermuth and E.J. Wurster, Phys. Lett. 29B, 455 (1969).

[20] D.R. Thompson and Y.C. Tang, Phys. Rev. C8, 1649 (1973).

[21] D.R. Thompson, Y.C. Tang and F.S. Chwieroth, Phys. Rev. C10, 987 (1974).

[22] H. Kanada, T. Kaneko, H. Nishioka and S. Saito, Prog. Theor. Phys. 63, 842 (1980).

[23] H. Kanada, T. Kaneko and Y.C. Tang, Nucl. Phys. A389, 285 (1982).

[24] H. Kanada, T. Kaneko, M. Nomoto and Y.C. Tang, Prog. Theor. Phys. 72, 369 (1984).

[25] H. Kanada, T. Kaneko, S. Saito and Y.C. Tang, Nucl. Phys. A444, 209 (1985).

[26] Yu.A. Kudeyarov, Yu.F. Smirnov and M.A. Chebotarev, Sov.Jour. Nucl.Phys. 4, 751 (1967).

[27] V.G. Neudatchin and Yu.F. Smirnov, Prog.Nucl.Phys. 10, 275 (1969).

[28] Il-T. Cheon, Phys. Lett. 30B, 81 (1969).

[29] A.K. Jain and N. Sarma, Phys. Lett. 33B, 271 (1970).

[30] Yu.A. Kudeyarov, I.V. Kurdyumov, V.G. Neudatchin and Yu.F. Smirnov, Nucl. Phys. A163, 316 (1971).

[31] J.C. Bergstrom, Nucl. Phys. A327, 458 (1979).

[32] J.C. Bergstrom, S.B. Kowalski and R. Neuhausen, Phys. Rev. C25, 1156 (1982).

[33] E.W. Schmid, Y.C. Tang and K. Wildermuth, Phys. Lett. 7, 263 (1963).

[34] J.M. Hansteen and H.W. Wittern, Phys. Lett. 24B, 381 (1967).

[35] H. Stowe, H.H. Hackenbroich and H. Hutzelmeyer, Z. Phys. 247, 95 (1971).

[36] A. Hasegawa and S. Nagata, Prog. Theor. Phys. 45, 1786 (1971).

[37] T. Mertelmeier and H.M. Hofmann, Nucl. Phys. A459, 387 (1986).

[38] T. Kajino, T. Matsuse and A. Arima, Nucl. Phys. A413, 323 (1984).

[39] T. Kajino, T. Matsuse and A. Arima, Nucl. Phys. A414, 185 (1984).

[40] Y.C. Tang in Topics in Nuclear Physics ed. T.T.S. Kuo and S.S.M. Wong (Springer-Verlag, 1981) p. 572.

[41] M.A. Nagarajan, and R.G. Lovas, Daresbury Laboratory, preprint DL/NUC/P107T/1980/.

[42] A.B. Volkov, Nucl. Phys. 74, 33 (1965).

[43] D.M. Brink and E. Boeker, Nucl. Phys. A91, 1 (1967).

[44] D.R. Thompson, M. LeMere and Y.C. Tang, Nucl. Phys. A286, 53 (1977).

[45] K.F. Pál et al., Nucl. Phys. A402, 114 (1983).

[46] R.S. Willey, Nucl.Phys. 40, 529 (1963).

[47] T. DeForest, Jr. and J.D. Walecka, Adv. in Phys. 15, 1 (1966).

[48] H. Überall, Electron Scattering from Complex Nuclei (Academic Press New York, 1971).

[49] C. Ciofi degli Atti, Prog.Part.Nucl.Phys. 3, 163 (1980).

[50] M. Bouten and M.C. Bouten, J.Phys.G: Nucl.Phys. 8, 1641 (1982).

[51] L. Tassie and F. Barker, Phys. Rev. 111, 940 (1958).

[52] H. Kanada, Q.K.K. Liu and Y.C. Tang, Phys. Rev. C22, 813 (1980).

[53] A.H. Wapstra and N.B. Gove, Nuclear Data Tables, 9, 265 (1971).

[54] R.C. Barrett and D.F. Jackson, Nuclear Sizes and Structure (Clarendon Press Oxford, 1977).

[55] T. Vertse, K.F. Pál and Z. Balogh, Comput. Phys. Commun. 27, 309 (1982).

[56] R.F. Frosch, J.S. McCarthy, R.E. Rand and M.R. Yearian, Phys. Rev. 160, 874 (1967).

[57] W. Czyz and L. Lesniak, Phys. Lett. 25B, 319 (1967).

[58] J. Borysowicz and D.O. Riska, Nucl. Phys. A254, 301 (1975).

[59] M. Radomski and D.O. Riska, Nucl. Phys. A274, 428 (1976).

[60] V.M. Muzafarov and V.E. Troitskii, Sov.J.Nucl. Phys. 33, 783 (1981).

[61] S. Galster, et al., Nucl. Phys. B32, 221 (1971).

[62] C.D. Buchanan and M.R. Yearian, Phys. Rev. Lett. 15, 303 (1965).

[63] D. Beneksas, D. Drickey and D. Frerejacque, Phys. Rev. 148, 1327 (1966).

[64] G.G. Simon, CH. Schmitt, and V.H. Walter, Nucl. Phys. A364, 285 (1981).

[65] D. Ganichot, B. Grossetete and D.B. Isabelle, Nucl.Phys. A178, 545 (1972).

[66] S. Auffret et al. Phys. Rev. Lett. 54,649 (1984).

[67] V.M. Muzafarov, V.E. Troitskii, and S.V. Trubnikov, Sov.J.Part. Nucl. 14, 467 (1983).

[68] F. Ajzenberg-Selove, Nucl. Phys. A413, 1 (1984).

[69] L.R. Suelzle, M.R. Yearian, and H. Crannel, Phys. Rev. 162, 992 (1967).

[70] G.C. Li, I. Sick, R.R. Whitney, and M.R. Yearian, Nucl. Phys. A162, 583 (1971).

[71] R.E. Brown and Y.C. Tang, Phys. Rev. 176, 1235 (1968).

[72] A.T. Kruppa, R.G. Lovas, R. Beck, and F. Dickmann, Phys. Lett. 179B, 317 (1986).

[73] M.A.K. Lodhi and R.B. Hamilton, Phys.Rev.Lett. 54, 646 (1984).

[74] F. Eigenbrod, Z. Phys. 228, 337 (1969).

[75] R. Yen et al., Nucl. Phys. A235, 135 (1974).

[76] J.C. Bergstrom and E.L. Tomusiak, Nucl. Phys. A262, 196 (1976).

[77] J.C. Bergstrom, U. Deutschmann, and R. Neuhausen, Nucl. Phys. A327, 439 (1979).

[78] Il-T. Cheon, S.J. Choi and M.T. Jeong, Phys. Lett. 144B, 312 (1984).

Table 1. The oscillator width parameters of the clusters using different interactions and models. The cluster stability condition is satisfied in the models DW and MW.

		$\beta_\alpha\,[fm^{-2}]$	$\beta_d\,[fm^{-2}]$
V2	CW	0.469	0.469
	DW	0.528	0.164
	MW	0.3159 0.6701 2.4367	0.0144, 0.7876 0.0602, 3.8191 0.23
BB1	CW	0.461	0.461
	DW	0.503	0.162
	MW	0.3275 0.6971 1.8139	0.0233, 1.2075 0.0957, 5.0659 0.3596
MN	CW	0.582	0.582
	DW	0.606	0.4374
	MW	0.3534 0.7917 2.6875	0.0411, 1.6028 0.1511, 5.7864 0.5151

Table 2. The binding energies (E_c) and rms radii ($\langle r_c^2 \rangle^{1/2}$) of the free clusters using different models and interactions. The experimental data are taken from Refs. 53 and 54.

		E_α [MeV]	$\langle r_\alpha^2 \rangle^{1/2}$ [fm]	E_d [MeV]	$\langle r_d^2 \rangle^{1/2}$ [fm]
V2	CW	-27.573	1.745	2.567	1.498
	DW	-27.957	1.666	0.579	2.284
	MW	-28.563	1.702	-0.608	3.530
BB1	CW	-27.097	1.757	2.523	1.507
	DW	-27.374	1.698	0.814	2.297
	MW	-28.460	1.702	-1.016	2.848
MN	CW	-24.633	1.606	0.189	1.391
	DW	-24.687	1.582	-0.1318	1.536
	MW	-25.595	1.620	-2.201	2.105
Exp.		-28.297	1.674±0.012	-2.225	2.095±0.006

Table 3. The space exchange parameters of the interactions V2 and BB1 and the u parameter of the force MN using different models. In the case of the force BB1 its attractive part was modified only.

V2	CW	0.57679
	DW	0.45781
	$D_\alpha D_d$	0.52166
	$G_\alpha D_d$	0.52032
	$G_\alpha G_d$	0.36593
BB1	CW	0.4012
	DW	0.30141
	$D_\alpha D_d$	0.38567
	$G_\alpha D_d$	0.37656
	$G_\alpha G_d$	0.14893
MN	CW	0.92555
	DW	0.9514
	$D_\alpha D_d$	0.9735
	$G_\alpha D_d$	0.9845
	$G_\alpha G_d$	1.3276

Table 4. Bulk properties of ^{6}Li using different models and interactions: binding energy (E), average of the energies of the first triplet 1^+, 2^+ and 3^+ states (E^*), rms radius of the ground state ($\langle r^2\rangle^{1/2}$), and reduced transition strength for transition leading to the first excited state ($B(E2, 3^+ \to 1^+)$). The experimental data are taken from Refs. 53,54 and 68.

		E [MeV]	E^* [MeV]	$\langle r^2\rangle^{1/2}$ [fm]	$B(E2, 3^+ \to 1^+)$ [e^2fm^4]
V2	CW	-26.48	3.34	2.66	10.86
	DW	-28.85	2.25	2.78	11.65
	$D_\alpha D_d$		2.65	2.65	9.57
	$G_\alpha D_d$	-30.64	2.82	2.65	9.49
	$G_\alpha G_d$		-0.166	2.94	7.83
BBl	CW	-26.05	3.29	2.66	10.86
	DW	-28.03	2.37	2.77	10.95
	$D_\alpha D_d$		3.46	2.65	9.02
	$G_\alpha D_d$	-30.95	3.41	2.67	9.06
	$G_\alpha G_d$		-3.38	2.83	7.83
MN	CW	-25.92	3.98	2.48	7.91
	DW	-26.29	3.85	2.50	8.05
	$D_\alpha D_d$		3.60	2.50	7.69
	$G_\alpha D_d$	-27.27	3.62	2.51	7.69
	$G_\alpha G_d$		0.42	2.51	5.24
Exp.		-31.99	3.6	2.56±0.1	10.9 ± 2.1

Figure captions

Fig. 1. Charge form factor of the ground state of the alpha particle: (a) in model DW (b) in model MW. The solid, dashed and dotted lines were calculated with interactions MN, V2, and BBl, respectively. The dots represent the data of Ref. 56.

Fig. 2. The invariant structure function $A(q^2)$ of the deuteron: (a) dotted line in CW model with force BBl, dashed-dotted line in DW model with force BBl, solid line in CW model with force MN, and dashed line in DW model with force MN (b) in model MW the solid, dashed, and dotted lines denote calculation with interaction MN, BBl, and V2, respectively. The dots represent the data of Ref. 61-64.

Fig. 3. The invariant structure function $B(q^2)$ of the deuteron. The notation is the same as in Fig.2. The dots represent the data of Refs. 63-66.

Fig. 4. Squared charge form factor of the ground state of ^{6}Li: (a) in model CW (b) in model DW. The solid, dashed, and dotted lines denote calculations with the interactions MN, V2, and BBl, respectively. The dots represent the data of Refs. 69 and 70.

Fig. 5. Squared charge form factor of the ground state of ^{6}Li in model MW: (a) with force V2 (b) with force BBl (c) with force MN. The solid, dashed, and dotted lines denote the results of the model $D_\alpha D_d$, $G_\alpha D_d$

and $G_{\alpha} G_{\delta}$, respectively. The dots represents the data of Ref. 69 and 70.

Fig. 6. Charge density of the ground state of ^{6}Li: (a) in model CW (b) in model DW. The solid line represents the charge density of Li et al.[70] fitted to the experiment. The dashed, dotted and dashed-dotted lines denote the result of the calculation with interactions V2, BB1 and MN, respectively.

Fig. 7. Charge density of the ground state of ^{6}Li in model MW: (a) with force V2 (b) with force BB1 (c) with force MN. The solid line represents the density of Li et al.[70] fitted to the experiment. The dashed, dotted and dashed-dotted lines denote the result of the models $D_{\alpha} D_{\delta}$, $G_{\alpha} D_{\delta}$, and $G_{\alpha} G_{\delta}$, respectively.

Fig. 8. Squared inelastic charge form factor of ^{6}Li: (a) in model CW (b) in model DW. The solid, dashed and dotted lines denote calculations with the interactions MN, V2, and BB1, respectively. The dots represent the data of Refs. 74-77.

Fig. 9. Squared inelastic charge form factor of ^{6}Li in model MW: (a) with force V2 (b) with force BB1 (c) with force MN. The solid, dashed and dotted lines denotes the results of the model $D_{\alpha} D_{\delta}$, $G_{\alpha} G_{\delta}$, and $G_{\alpha} G_{\delta}$, respectively. The curves of the models $D_{\alpha} D_{\delta}$ and $G_{\alpha} G_{\delta}$ concide in the Figs. 9a and 9b. The dots represent the data of Ref. 74-77.

Fig.10. Squared magnetic form factor of the ground state of ^{6}Li: (a) in model CW (b) in model DW. The solid, dashed and dotted lines denote calculations with the interactions MN, V2, and BB1, respectively. The dots represent the data of Ref. 32.

Fig. 11. Squared magnetic form factor of the ground state of ^{6}Li in model MW: (a) with force V2 (b) with force BB1 (c) with force MN. The solid, dashed and dotted lines denotes the results of the model $\underline{\underline{D}}\,\underline{\underline{D}}$, $\underline{\underline{G}}\,\underline{\underline{D}}$, and $\underline{\underline{G}}\,\underline{\underline{G}}$, respectively. The dots represent the data of Ref. 32.

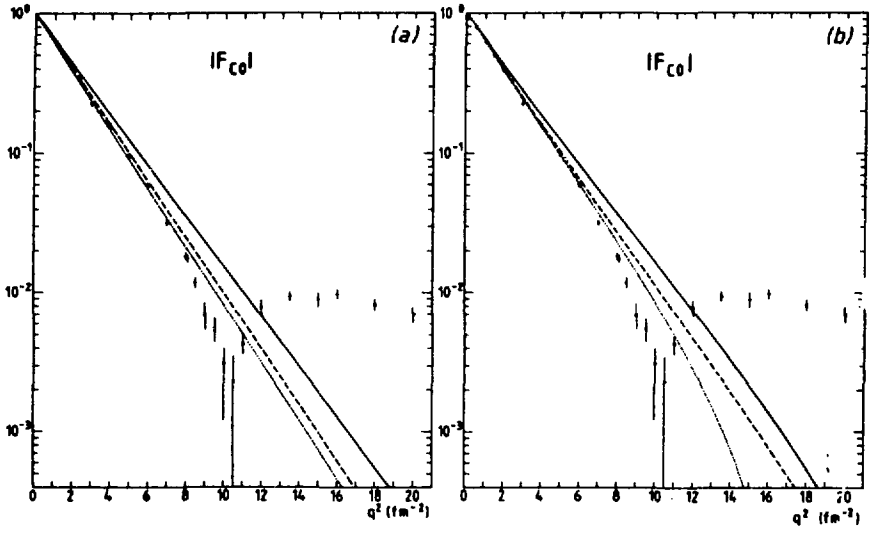

Fig. 1

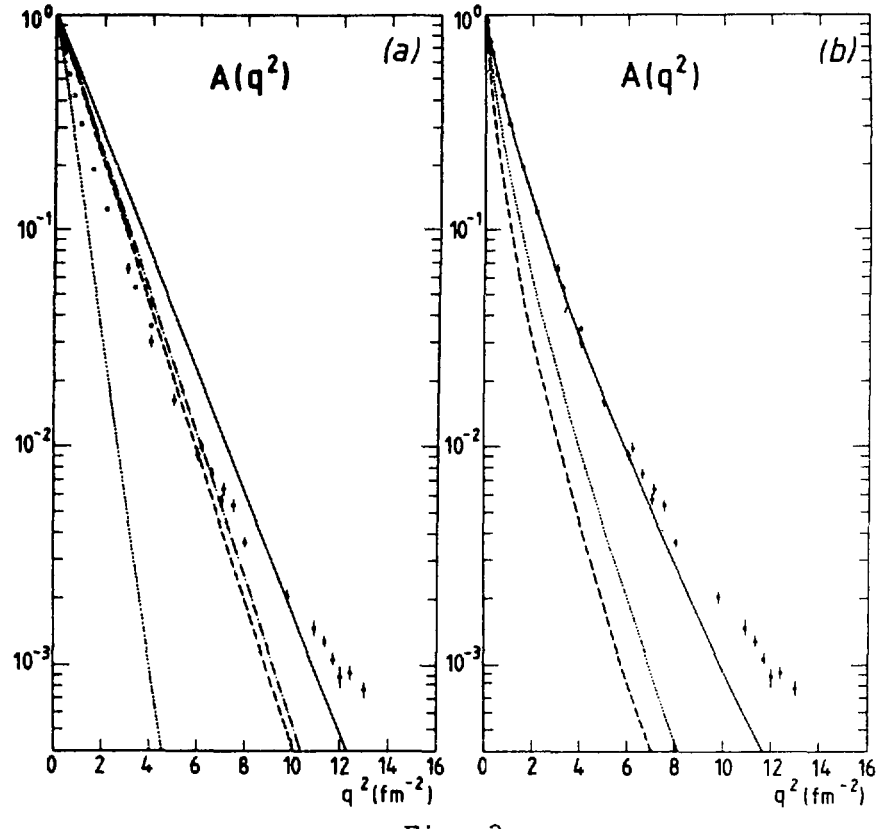

Fig. 2

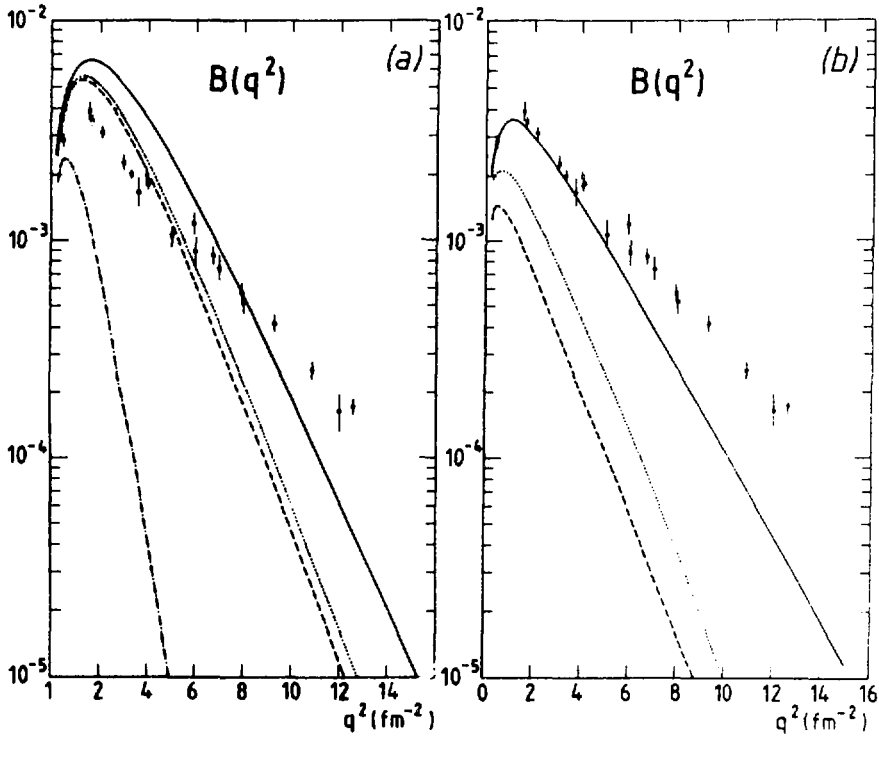

Fig. 3

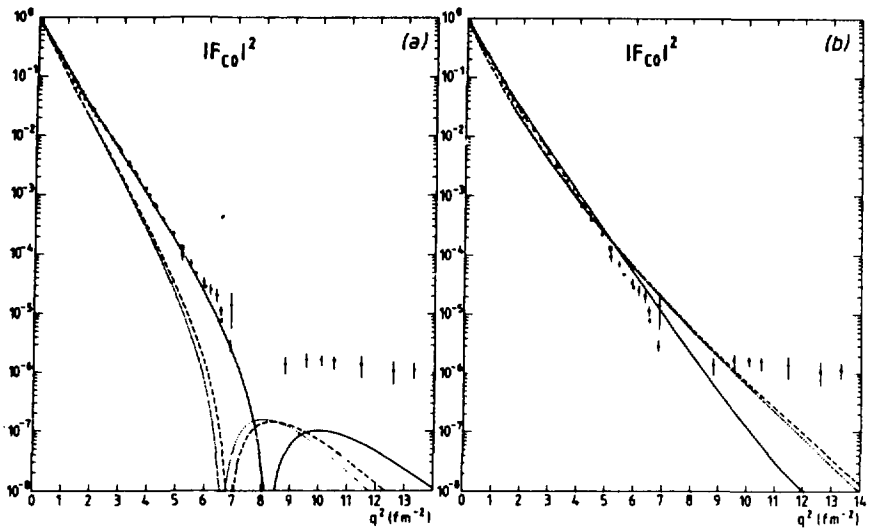

Fig. 4

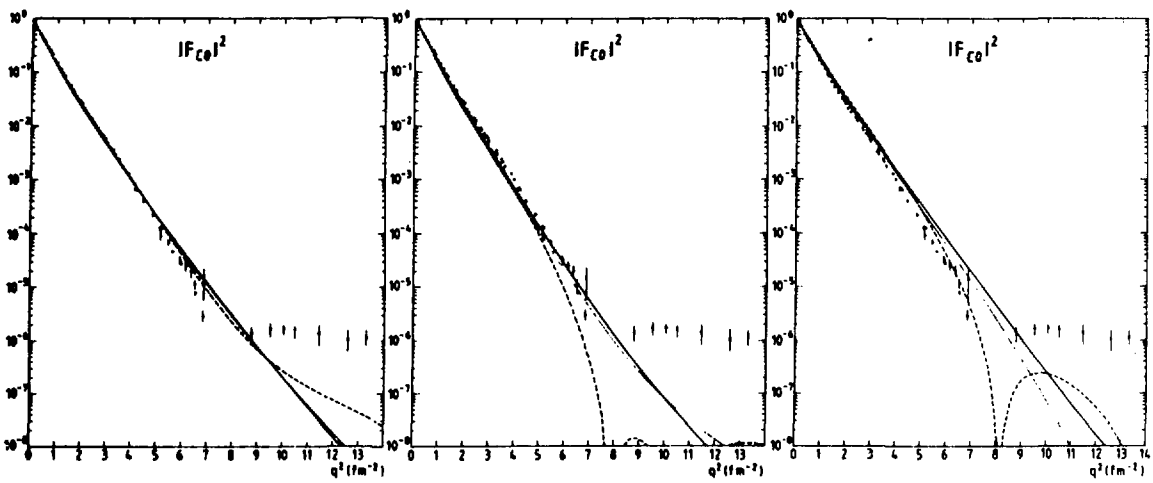

Fig. 5

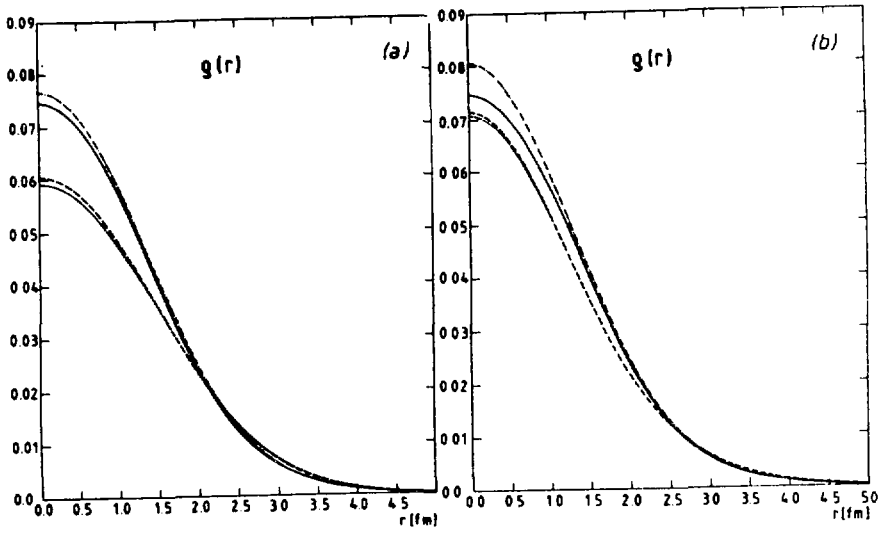

Fig. 6

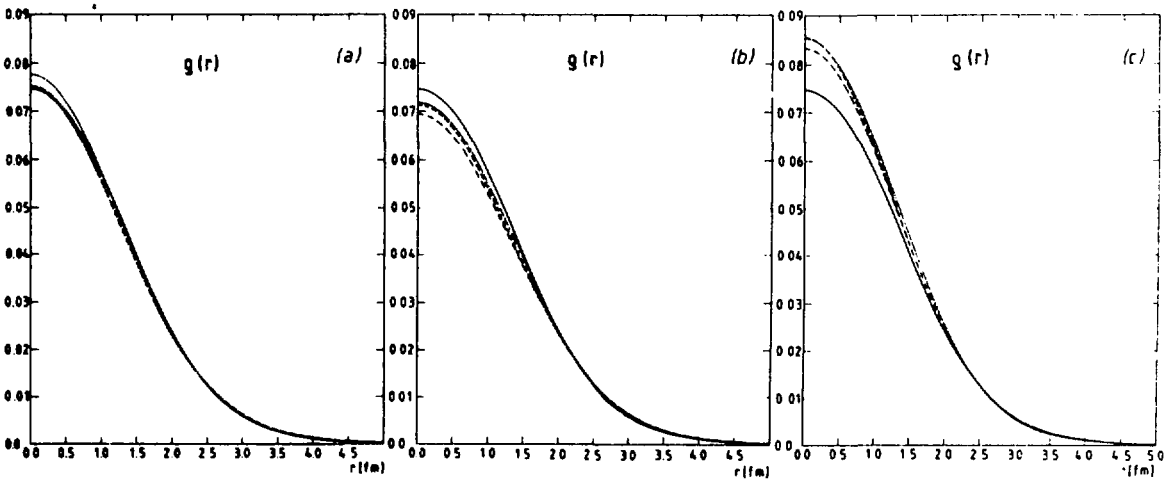

Fig. 7

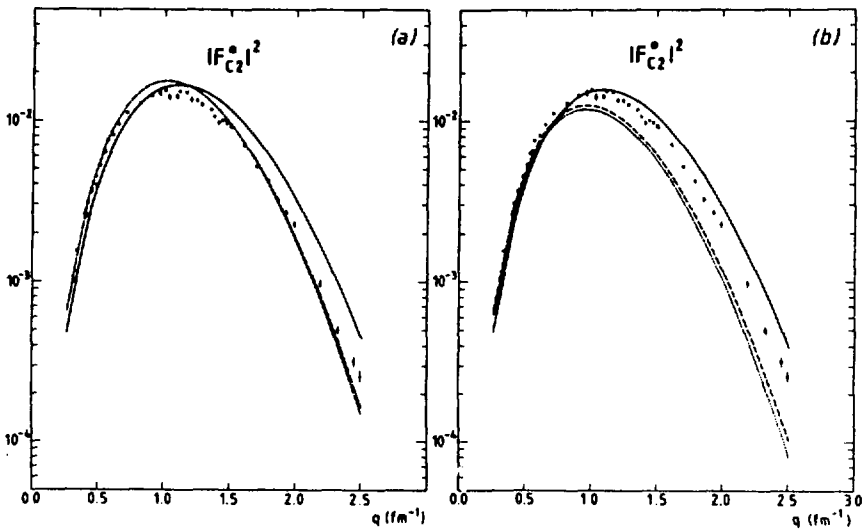
(a)
(b)
$|F^{*}_{C2}|^2$
10^{-2}
10^{-3}
10^{-4}
0.0
0.5
1.0
1.5
2.0
2.5
3.0
q (fm^{-1})

Fig. 8

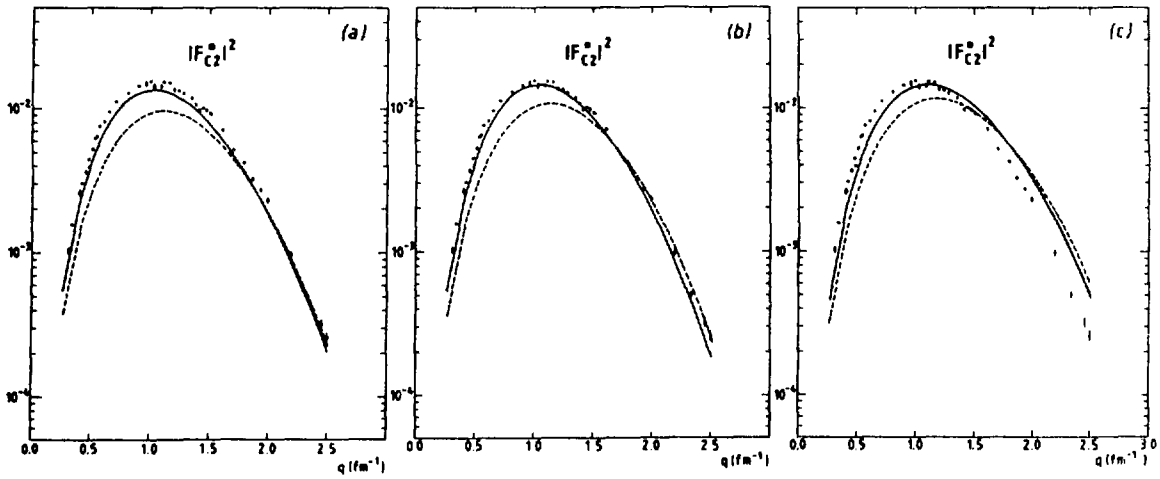
(a)
(b)
(c)
$|F^{*}_{C2}|^2$
10^{-2}
10^{-3}
10^{-4}
0.0
0.5
1.0
1.5
2.0
2.5
3.0
q (fm^{-1})

Fig. 9.

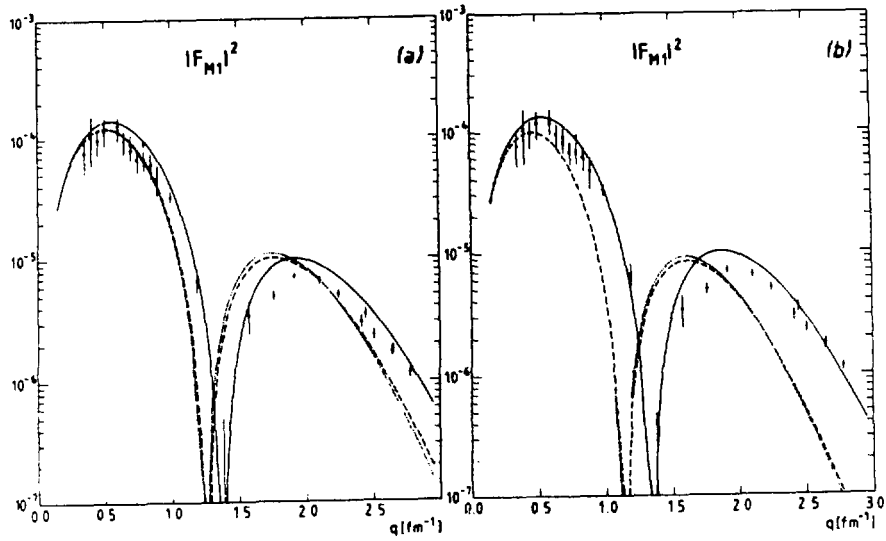

Fig. 10

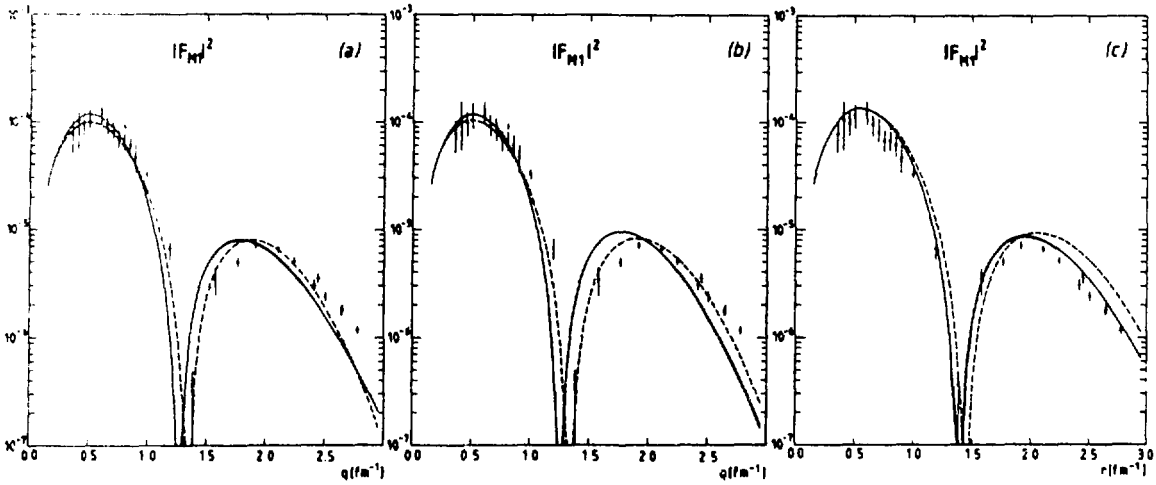

Fig. 11